



Cite this article: Pike SD, Weller AS. 2015 Organometallic synthesis, reactivity and catalysis in the solid state using well-defined single-site species. *Phil. Trans. R. Soc. A* **373**: 20140187.
<http://dx.doi.org/10.1098/rsta.2014.0187>

One contribution of 18 to a discussion meeting issue 'The new chemistry of the elements'.

Subject Areas:
organometallic chemistry

Keywords:
solid state, organometallic, reactivity, catalysis

Authors for correspondence:

Sebastian D. Pike
e-mail: s.pike@imperial.ac.uk
Andrew S. Weller
e-mail: andrew.weller@chem.ox.ac.uk

[†]Present address: Imperial College London,
South Kensington Campus, London SW7 2AZ,
UK.

Organometallic synthesis, reactivity and catalysis in the solid state using well-defined single-site species

Sebastian D. Pike[†] and Andrew S. Weller

Department of Chemistry, University of Oxford, Mansfield Road, Oxford UK1 3TA, UK

Acting as a bridge between the heterogeneous and homogeneous realms, the use of discrete, well-defined, solid-state organometallic complexes for synthesis and catalysis is a remarkably undeveloped field. Here, we present a review of this topic, focusing on describing the key transformations that can be observed at a transition-metal centre, as well as the use of *well-defined* organometallic complexes in the solid state as catalysts. There is a particular focus upon gas–solid reactivity/catalysis and single-crystal-to-single-crystal transformations.

1. Introduction

Organometallic chemistry, rigorously defined by the chemical synthesis and reactivity of molecules with metal–carbon bonds, is a vibrant area of research with a large variety of practical applications [1]. For example, organometallic complexes are commonly used as catalysts for the production of commodity chemicals, materials such as polymers, and in fine chemical synthesis and medicinal chemistry discovery [1,2]. The majority of discoveries in the area have been performed in the solution phase, with studies in the solid state generally often reserved only for structural analysis; for example, single-crystal X-ray crystallography and, to a significantly lesser extent, solid-state nuclear magnetic resonance spectroscopy. By contrast to the solution phase, studies on the synthesis of, and catalysis using, organometallic complexes in the solid phase have attracted significantly less attention, even though there are potential benefits to this approach, such as: improved

© 2015 The Authors. Published by the Royal Society under the terms of the Creative Commons Attribution License <http://creativecommons.org/licenses/by/4.0/>, which permits unrestricted use, provided the original author and source are credited.

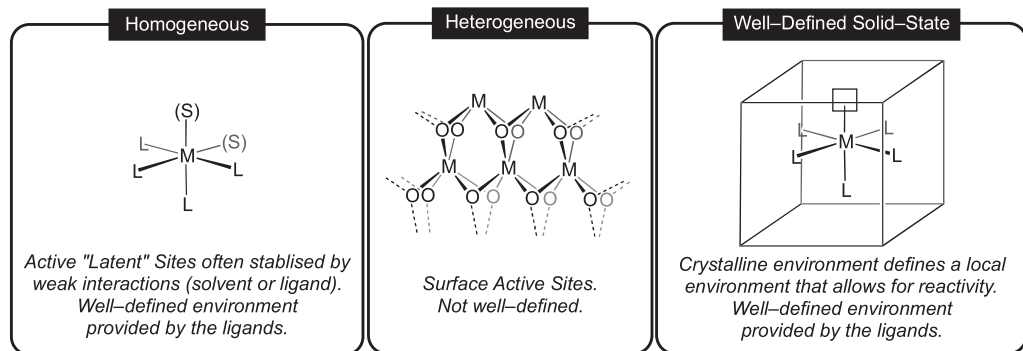


Figure 1. Molecular, heterogeneous and well-defined solid-state organometallic motifs.

selectivities in synthesis that comes from spatially confined environments, improved isolated yields of products and the attenuation of decomposition pathways allowing for products that might be kinetically unstable in solution to be observed in the solid state.

Heterogeneous catalysis using the surfaces of metals or ionic platform materials is a well-researched area of chemistry with many industrial uses [3–5]. However, the mechanism of the binding, catalytic steps and product release may be multifarious or difficult to resolve when using such an extended material. There may also be a limited number of 'active sites' for catalysis. By contrast, homogeneous catalysis tends to be significantly more well defined, allowing for the mechanistic pathways to be readily probed using a wide variety of analytical and kinetic techniques, and often uses a single active metal centre that can be tuned by modifying the supporting ligand set, often with exquisite control with regard to reactivity and selectivity [1,6]. This greater degree of molecular control using a single-site catalyst can thus allow for stereoselective or regiospecific reactivity to be more readily tuned [7,8]. Moreover, the solvent (or sometimes ligand, for example $M \cdots H-C$ agostic interactions [9]) can play a role in stabilizing the active site(s) on the metal often necessary for reactivity, by forming weak interactions that are readily replaced by incoming substrates, so-called 'virtual' [10] or operationally unsaturated vacant sites [11].

Acting as a bridge between the heterogeneous and homogeneous realms, the use of discrete, well-defined, solid-state organometallic complexes for synthesis and catalysis is a remarkably undeveloped field (figure 1) [12–14]. In principle, if using reagents in the gas phase that can penetrate the lattice (i.e. a solid–gas reaction), or when in contact with a solvent that will not dissolve the organometallic species but solvates substrates and products, the active organometallic species can partake in the same processes observed in the solution phase, such as ligand substitution, oxidative addition, reductive elimination and insertion reactions. These resulting single-site catalysts thus bring together the benefits of heterogeneous catalysis (i.e. recyclability and easy removal from the reaction mixture) with the potential for intimate control over the transformations that the metal–ligand environment promotes in a homogeneous system [15,16]; for example, the high degrees of selectivity and mechanistic control associated with a well-defined metal–ligand environment, while harnessing the particular benefits of a solid-state environment. Further advantages of such an approach in catalysis include the simple separation of products from the catalyst [17,18], while avoiding the use of solvents in such solid–gas processes has potential economic and environmental benefits. Finally, and perhaps most excitingly, such a methodology potentially allows for the study of organometallic species without the complications of unwanted reactivity with the solvent. Such species, if being both low coordinate and of low electron count, could well be intermediates in catalytic processes that are often implicated but not observed in solution-phase chemistry. Solid-state reactivity using well-defined single-site organometallic complexes thus potentially allows for the isolation of otherwise unstable complexes, kinetically trapped in the solid state.

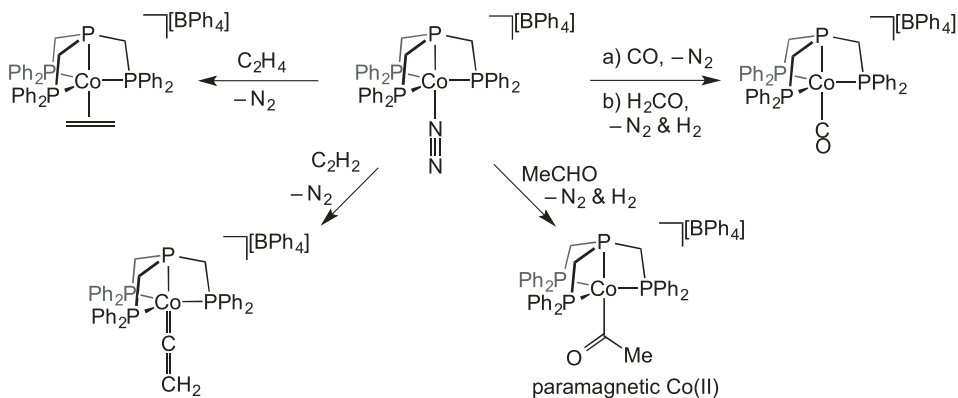
2. Scope of this review

In this review, we discuss selected examples of solid-state organometallic synthetic chemistry and catalysis, focusing on describing the key transformations that can be observed, as well as the use of *well-defined* organometallic complexes in the solid state as catalysts. In particular, we focus on gas–solid reactivity, as this presents the ideal opportunity to explore transformations and catalysis while retaining the crystalline integrity (i.e. single-crystal-to-single-crystal transformations)—which is important for both structural studies (i.e. molecular structures by single-crystal X-ray diffraction) and reactivity (well-defined voids and channels in the lattice to allow for reactivity). We do not attempt to comprehensively review the solid-state organometallic chemistry associated with simple ligand substitution reactions where crystallinity is lost [12], isomerization reactions [19] or mechanochemical transformations [12,19–23]. In addition, the vibrant field of metal–organic framework materials and the encapsulation of active species inside the cavities of these materials is only discussed in passing where appropriate [24,25]. Likewise, we do not cover photocrystallographic techniques that allow for the determination of molecular structures of metastable species generated in the crystal photochemically. This technique has been used, for example, to study linkage isomerization in transition-metal complexes with nitrosyl, dinitrogen, sulfur dioxide and nitrite ligands, when photoactivated by light of an appropriate wavelength [26]; or photoinduced spin-crossover transitions, the structural consequences of which can be measured by photocrystallography [27]. Related to this is the development of ‘crystalline molecular flasks’ [28,29] in which self-assembled cages (e.g. from Pd^{2+} ions and triazene ligands) can be used to encapsulate and stabilize highly reactive complexes formed by photo-irradiation, such as the photodissociated complex $(\eta^5\text{-C}_5\text{H}_5\text{Me})\text{Mn}(\text{CO})_2$ [30].

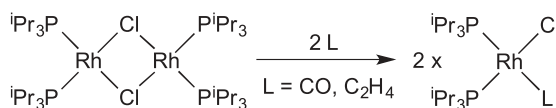
This is not the first time the general area of solid-state organometallic chemistry has been reviewed. An excellent in-depth account by Coville & Cheng [12] presented the area of solid-state organometallic chemistry in 1998 with updates with regard to isomerization reactions [19] and organometallic reactions that occur in the melt [31]. A recent (2011), short, highlight article by van der Boom [32] describes molecular single-crystal-to-single-crystal transformations in coordination chemistry. Our intention is that this review builds on these contributions, in particular bringing together both recent and older publications on solid–gas reactivity.

3. General considerations

For reactivity to occur in the solid state, the reagents must be able to penetrate the extended structure and access the metal sites; and this suggests that porosity within the extended solid structure will aid reaction [13,33]. The idea of a ‘reaction cavity’ was pioneered by Cohen & Schmidt [34], who proposed that reactions in the solid state occur with the least amount of molecular movement possible. There is, however, good evidence of limited molecular movement within the solid state from X-ray diffraction studies, in particular the rotation of CH_3 , CF_3 and C_5H_5 groups [35]. The nevertheless constrained environments within a solid structure open up the possibilities of added reaction selectivity, potentially different from that observed in solution. For example, if a reaction cavity could be designed to be chiral then asymmetric reactivity may also be possible [36]. As solid-state reactions proceed, the products will replace the reagents. This generally occurs from the surface downwards, and Kaupp [37] has proposed the idea of ‘phase rebuilding’ where reaction direction is determined by crystallographic faces, and lattice reconstruction occurs over thousands of angstroms at a time. The kinetics of solid-state reactions have proved difficult to measure owing to their inherent complexity, as the reaction may take place at different rates upon the surface and within the interior of a crystalline material. For example, Caulton and co-workers [38] proposed that changes in molecular shape on reaction induce strain in a crystalline material, which in turn promotes micro-cracking. Such cracks will expose more of the interior of the crystal to the gaseous reagent and increase reaction rate. When



Scheme 1. Solid-state gas exchange reactions facilitated by labile N_2 ligands.



Scheme 2. Solid–gas reactivity of a dimeric species to afford monomeric complexes.

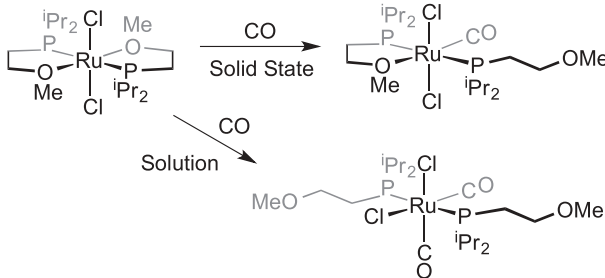
little change in shape occurs the crystals may become ‘passivated’ by a surface layer of the product, slowing further reactivity.

4. Stoichiometric solid–gas reactions

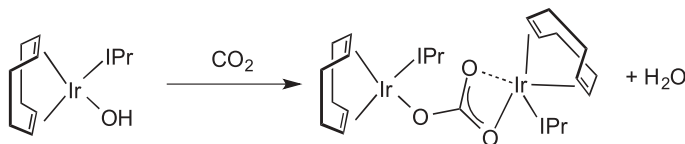
A very early example of solid-state organometallic synthesis using solid–gas techniques was reported in the 1960s when the oxidative addition of various HX gases (HF , HCl , HBr , HI and H_2S) to Vaska-type complexes $\text{IrX}'(\text{CO})(\text{PPh}_3)_2$ ($\text{X}'=\text{Cl}, \text{Br}, \text{I}, \text{SCN}$) was reported to form *trans*- $\text{Ir}(\text{PPh}_3)_2(\text{X}')(\text{CO})(\text{H})(\text{X})$ [39]. Similarly, addition of I_2 to $\text{Pt}(\text{acac})_2$ ($\text{acac}=\text{acetylacetone}$) forms the oxidative addition product *trans*- $\text{PtI}_2(\text{acac})_2$ [40]. More recently, Brammer and co-workers [41–43] have shown that the reaction of *trans*- $[\text{CuCl}_2(n\text{-X-C}_5\text{H}_4\text{N})_2]$ ($n=3, 4$; $\text{X}=\text{Cl}, \text{Br}$) with HCl gas to form $[\text{n-X-C}_5\text{H}_4\text{NH}]_2[\text{CuCl}_4]$ requires breaking of two $\text{Cu}-\text{N}$ bonds to form $\text{Cu}-\text{Cl}$ bonds and $\text{N}-\text{H}$ bonds. These reactions have been monitored by powder diffraction, including *in situ* powder synchrotron diffraction [41], showing that microcrystalline products are formed.

Organometallic stoichiometric reactions with gaseous reagents were extensively studied by Bianchini in the 1990s. For example, the displacement of labile N_2 from $[\{\kappa^4\text{-P}(\text{C}_2\text{H}_4\text{PPh}_3)_3\}\text{Co}(\text{N}_2)][\text{BPh}_4]$ by various gases was studied in a solid–gas reaction (scheme 1) [44]. It was proposed that small gaseous reagents could penetrate the crystal lattice of $[\text{BPh}_4]^-$ anions by dissolving in the hydrophobic regions formed by the tetraphos ligand backbone and anion phenyl groups. As is shown later (§5), displacement of a labile N_2 also occurs in single-crystal-to-single-crystal transformations.

An interesting case of ligand displacement, in as much as that cleavage of a dimer is occurring in the solid state, comes from the reaction shown in scheme 2 in which Werner and co-workers [45] reported that addition of CO or ethene to a chloride-bridged $\text{Rh}(\text{I})$ dimer resulted in the generation of monomeric species, where two dative $\text{Rh}-\text{Cl}$ bonds had been cleaved by CO or ethene. Other examples of ligand displacement in the solid state have been reported. Werner and co-workers reported that addition of CO to a Rh -complex that contains a hemilabile [46,47] phosphine–ether ligand results in displacement of one Rh -ether



Scheme 3. Hemilabile ligand displacement in the solid state.



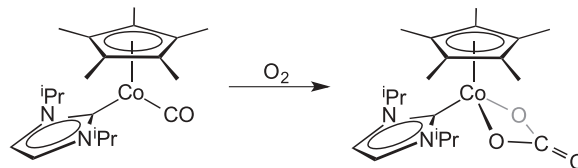
Scheme 4. CO_2 fixation using an Ir-hydroxide.

linkage, whereas a dicarbonyl will form in the analogous solution-phase reaction (scheme 3) [45]. Addition of CO to $\text{Rh}(\text{PPh}_3)_3(\text{OAr})$ (e.g. Ar = C_6Cl_5) in the solid state results in an intermediate, tentatively described as five-coordinate $\text{Rh}(\text{PPh}_3)_3(\text{OAr})(\text{CO})$, from which washing of the solid with ether removes PPh_3 to afford *trans*- $\text{Rh}(\text{PPh}_3)_2(\text{OAr})(\text{CO})$ [48]. Related five-coordinate species can be isolated from addition of CO in the solid state to square planar complexes such as $[\text{Ir}(\text{COD})(\text{PPh}_3)(\text{PhCN})][\text{ClO}_4]$ to give, for example, $[\text{Ir}(\text{COD})(\text{PPh}_3)(\text{CO})_2][\text{ClO}_4]$ via loss of PhCN [49]. Milstein and co-workers [50] have shown that CO can bind reversibly to a 16-electron Rh(I) nitrosyl pincer complex, in which an equilibrium is established between a five-coordinate, CO-bound, and four-coordinate, CO-free, complex. Concomitant with this addition of CO is the change in NO binding mode from linear to bent, as measured by infrared (IR) spectroscopy.

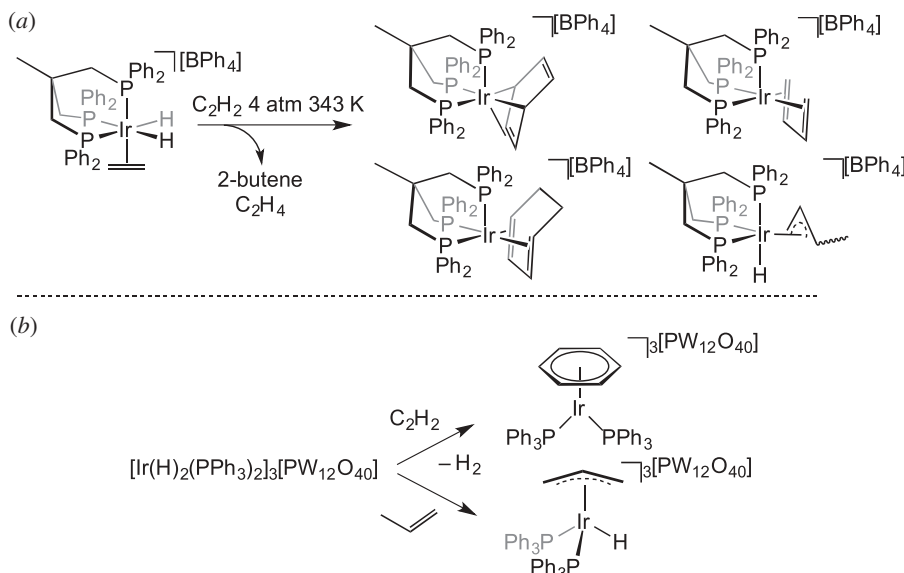
The reversible addition of CO_2 to the rhodium and iridium complexes $\text{M}(\text{CO})(\text{PPh}_3)_2(\text{OH})$ was reported by Flynn & Vaska [51], although the nature of the $\text{M}\cdots\text{CO}_2$ interaction was not clarified. Very recently, Nolan and co-workers [52] have reported that CO_2 rapidly (2 min) inserts into the O–H bond of $\text{Ir}(\text{COD})(\text{IPr})\text{OH}$ ($\text{IPr} = 1,3\text{-di-isopropyl-imidazolin-2-ylidene}$) in a solid-gas reaction to form a bimetallic carbonate, $[\text{Ir}(\text{COD})(\text{IPr})_2(\mu, \kappa^1 : \kappa^2-\text{CO}_3)]$, scheme 4, with the concomitant elimination of water [$\text{IPr} = 1,3\text{-bis(isopropyl)imidazol-2-ylidene}$].

A related carbonate complex that comes from the aerobic oxidation of $(\eta^5\text{-C}_5\text{Me}_5)\text{Co}(\text{IPr})(\text{CO})$ to form a carbonato complex $(\eta^5\text{-C}_5\text{Me}_5)\text{Co}(\text{IPr})(\kappa^2\text{-CO}_3)$ was reported by Radius and co-workers [53]. This process occurs rapidly in air, both in solution and in the solid phase (scheme 5).

Addition of alkynes and alkenes to a metal complex may result in olefin oligomerization through C–H and C–C coupling processes, common transformations in solution-phase organometallic chemistry [1]. Bianchini *et al.* [54,55] demonstrated that addition of C_2H_2 to $[\text{Ir}(\text{triphos})(\text{C}_2\text{H}_4)(\text{H})_2][\text{BPh}_4]$ [triphos = $(\text{Ph}_2\text{PCH}_2)_3\text{CCH}_3$] in the solid state leads to various products, including benzene and butadiene complexes (scheme 6a). Siedle & Newmark [56] have demonstrated trimerization of C_2H_2 with $[\text{Ir}(\text{H})_2(\text{PPh}_3)_2]_3[\text{PW}_{12}\text{O}_{40}]$ to form a benzene complex, whereas C–H activation of propene with the same organometallic starting material forms an allyl complex (scheme 6b). Related transformations in which bound ethene in a Rh(I) tripyrazolylhydroborate complex undergoes C–H and C–C bond-forming processes to form allylic species have been reported by Carmona and co-workers [57]. C–Br activation in an η^2 -azobenzene ligand coordinated to a $\{\text{Pt}(\text{PEt}_3)_2\}$ fragment occurs in the solid state to give the corresponding Pt-aryl-halide [58]. The oxidative addition of a



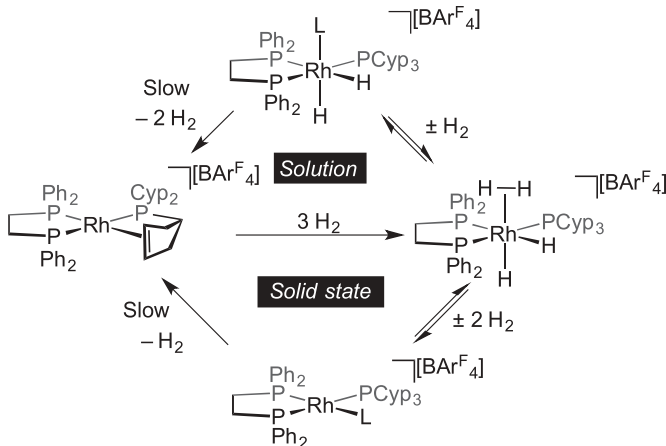
Scheme 5. Aerobic oxidation to a carbonyl to form carbonate complex.



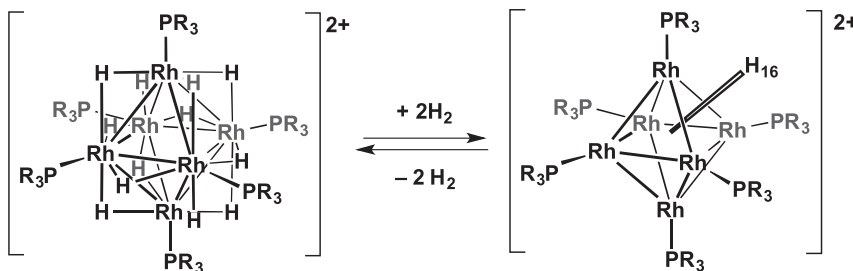
Scheme 6. (a,b) Reaction of cationic iridium complexes with alkenes and alkynes in the solid state resulting in C–C couplings and/or C–H activation.

C–Cl bond is reported in the solid-state transformation of the zwitterionic Rh(I) η^6 -arene complex $[\text{Rh}(\text{iBu}_2\text{PCH}_2\text{CH}_2\text{P}^{\text{i}}\text{Bu}_2)\{(\eta^6\text{-C}_6\text{H}_3\text{Cl}_2)\text{BAr}_3^{\text{Cl}}\}]$ ($\text{Ar}_3^{\text{Cl}} = 3,5\text{-C}_6\text{H}_3\text{Cl}_2$) into the dimeric Rh(III) complex $[\text{Rh}(\text{iBu}_2\text{PCH}_2\text{CH}_2\text{P}^{\text{i}}\text{Bu}_2)(\text{Cl})\{(\text{C}_6\text{H}_3\text{Cl})\text{BAr}_3^{\text{Cl}}\}]_2$ [59]. Interestingly, this process generates two isomers in the solid state, whereas the same process in solution only accesses the thermodynamic isomer. Bond isomerizations in the solid state, involving C–C cleavage, between Ru-alkynylketones and Ru-vinylidenes have been followed using IR spectroscopy, and kinetic data were obtained for this transformation. This is a very rare example of such an analysis of reactivity in solid-state organometallic chemistry, and, from these data, the authors propose a mechanism controlling the reaction that invokes nucleation and nuclei growth rather than diffusion, chemical reaction or phase boundary-controlled steps [60].

Reversible hydrogen addition to metal complexes is of considerable interest with regard to processes such as hydrogenation, hydrodesulfurization and hydrogen storage applications [1]. The reversible addition of three molecules of hydrogen to $[(\text{Ph}_2\text{PCH}_2\text{CH}_2\text{PPh}_2)\text{Rh}(\kappa, \eta_{\text{P},\text{C}}^2 \text{PCy}_2(\eta^2\text{-C}_5\text{H}_7))]\text{BAr}_4^{\text{F}}$ ($\text{Cyp} = \text{C}_5\text{H}_9$, $\text{Ar}^{\text{F}} = 3,5\text{-C}_6\text{H}_3(\text{CF}_3)_2$) to form $[(\text{Ph}_2\text{PCH}_2\text{CH}_2\text{PPh}_2)\text{Rh}(\text{PCy}_3)(\text{H})_2(\text{H}_2)]\text{BAr}_4^{\text{F}}$ has been reported, in which a dihydrogen ligand is coordinated, and the phosphine–alkene ligand has been hydrogenated [61]. In the solid phase, the product loses two molecules of hydrogen under application of a vacuum to form a red intermediate proposed to be the Rh(I) complex $[\text{Rh}(\text{Ph}_2\text{PCH}_2\text{CH}_2\text{PPh}_2)(\text{PCy}_3)]\text{BAr}_4^{\text{F}}$, in which an agostic interaction from the phosphine is proposed. This red intermediate then slowly loses a further equivalent of H_2 via an alkyl dehydrogenation (C–H activation and β -elimination) to reform



Scheme 7. Reversible addition of hydrogen and C–H activation in solution and the solid state. L = agostic or solvent interactions.

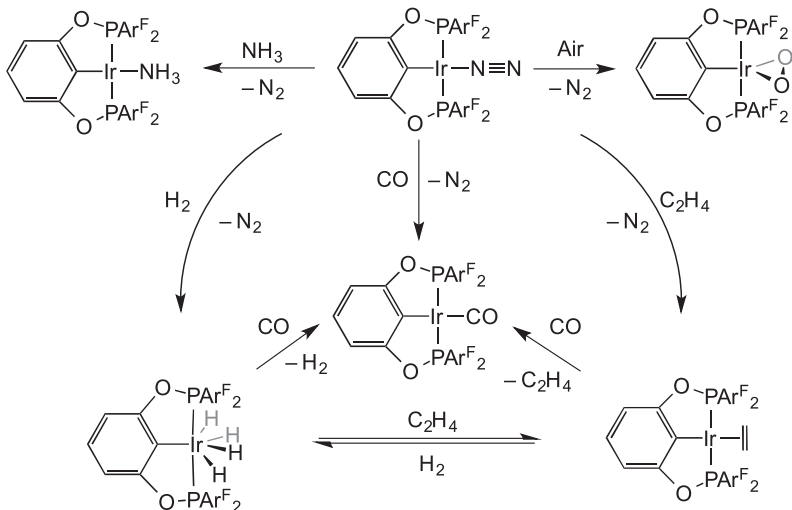


Scheme 8. Reversible H₂ addition to [Rh₆(ⁱPr₃)₆(H)₁₂][BAr₄^F]₂. R = ⁱPr.

[(Ph₂PCH₂CH₂PPh₂)Rh{ κ , $\eta^2_{P,C}=\text{C}$ }PCyp₂($\eta^2\text{-C}_5\text{H}_7$)][BAr₄^F]. In solution, no red Rh(I) intermediate is observed, and removal of the dihydrogen ligand under vacuum results, instead, in a Rh(III) dihydride (scheme 7).

The simple reversible addition of dihydrogen to monometallic [62] and multi-metallic cluster [63–66] species in the solid state has been reported by a number of groups. In these instances, the H₂-free complexes are often electronically unsaturated and stabilized by bulky ligands around the metal centre(s). An example shown in scheme 8 is the reversible addition of two molecules of H₂ to the cluster [Rh₆(ⁱPr₃)₆H₁₂][BAr₄^F] to give [Rh₆(ⁱPr₃)₆H₁₆][BAr₄^F] [67]. Related coordinate unsaturation in clusters enabled via loss of a weakly bound ligand in the solid state (such as NCMe) allows for solid–gas reactivity of Os₃(CO)₁₁L (L = NCMe) with CO, NH₃ and H₂ [68].

Deliberate installation of coordinate and electronic unsaturation at a metal centre means that solid–gas reactions can be made particularly facile. Caulton and co-workers have reported that 16-electron Ru(CO)₂(P^tBu₂Me)₂ adds H₂, Cl₂ or O₂ to give the corresponding 18-electron complexes *cis,cis,trans*-Ru(H)₂(CO)₂(P^tBu₂Me)₂, *cis,cis,trans*-Ru(Cl)₂(CO)₂(P^tBu₂Me)₂ and Ru($\eta^2\text{-O}_2$)(CO)₂(P^tBu₂Me)₂, respectively. Interestingly, reaction with HSiMe₃ gave the dihydride Ru(H)₂(CO)₂(P^tBu₂Me)₂ dissolved in liquid Me₃SiSiMe₃, formed by a dehydrocoupling process. Reaction with CO is particularly slow, and this is postulated to be due to the fact that the product, Ru(CO)₃(P^tBu₂Me)₂, is a similar size to the organometallic reactant, and this results in surface passivation rather than the fracturing of the crystal (and concomitant faster ingress of gas) that is suggested to occur when product and starting material geometries are different [38]. The electronically and coordinatively unsaturated complex



Scheme 9. SC–SC transitions using Ir–pincer complexes. $\text{Ar}^F = 2,4,6\text{-C}_6\text{H}_2(\text{CF}_3)_3$.

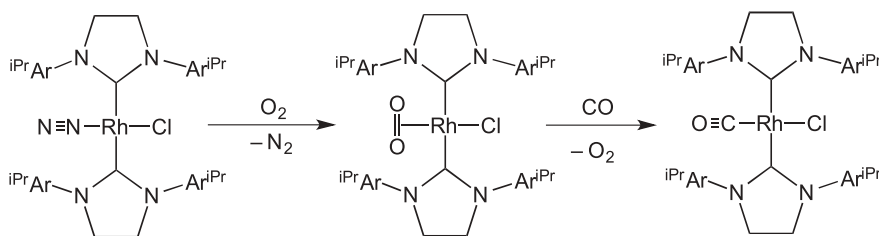
$[(\eta^5\text{-C}_5\text{Me}_5)\text{Ru}(\text{Me}_2\text{NCH}_2\text{CH}_2\text{NMe}_2)][\text{BAR}_4^F]$ adds H_2 , N_2 , O_2 , CO and ethylene in the solid state, with the latter shown to be reversible. These new complexes (except the CO adduct) were unstable in solution and were characterized by elemental analysis [69].

5. Single-crystal-to-single-crystal transformations

A single-crystal-to-single-crystal (SC–SC) transition is one in which crystallinity is retained throughout a reaction, allowing the product to be characterized directly by single-crystal X-ray crystallography without recourse to recrystallization from solution [32]. For crystallinity to be retained, only a very small structural reorganization can be tolerated to avoid the break-up of the lattice. Crystal size also probably affects reaction time in SC–SC transitions because of surface area to volume ratio implications. Molecular designs that enable such transitions to take place involve use of bulky ligands or anions which dominate the packing and thus can create a rigid, porous, structure in which smaller movements around the metal centre are made possible [13,70]. SC–SC reactions present excellent possibilities for selectivity to be controlled within a solid-state environment, as the reaction cavity necessarily must remain well defined throughout to preserve crystallinity.

If gaseous reagents require access to the interior of the crystal then empty or partially filled channels throughout the lattice may be necessary [33]. This was suggested by Brookhart and co-workers [13], who noted the channels of disordered toluene throughout the crystalline lattice of $(\text{POCOP})\text{IrL}$ ($\text{POCOP} = 1,3\text{-[OP}\{2,4,6\text{-C}_6\text{H}_2(\text{CF}_3)_3\}_2\}_2\text{C}_6\text{H}_3$, $\text{L}=\text{N}_2, \text{CO}, \text{NH}_3, \text{C}_2\text{H}_4, \text{O}_2$). They reported a series of SC–SC gas transfer reactions using this system (scheme 9). Interestingly, the precursor complex studied ($\text{L}=\text{N}_2$) is stable under vacuum, but readily reacts with more strongly binding gases, which suggests that an associative mechanism for gas exchange is operating within the interior of the crystal. These SC–SC transformations presumably occur as the packing in the lattice is dominated by the large tris-(CF_3) substituted aryl groups on the pincer ligand, meaning that changes in the ancillary ligands around Ir (e.g. CO for N_2) result in minimal structural reorganization.

Such transitions can also be reversible. van Koten and co-workers [71,72] reported the reversible addition of SO_2 to $(\text{NCN})\text{PtCl}$ ($\text{NCN}=\text{C}_6\text{H}_2\text{-5-(OH)-1,3-(CH}_2\text{NMe}_2)_2$), which induced significant changes in the geometry of the metal centre, from square planar to pseudo-square pyramidal, and remarkably such a large structural change does not result in the



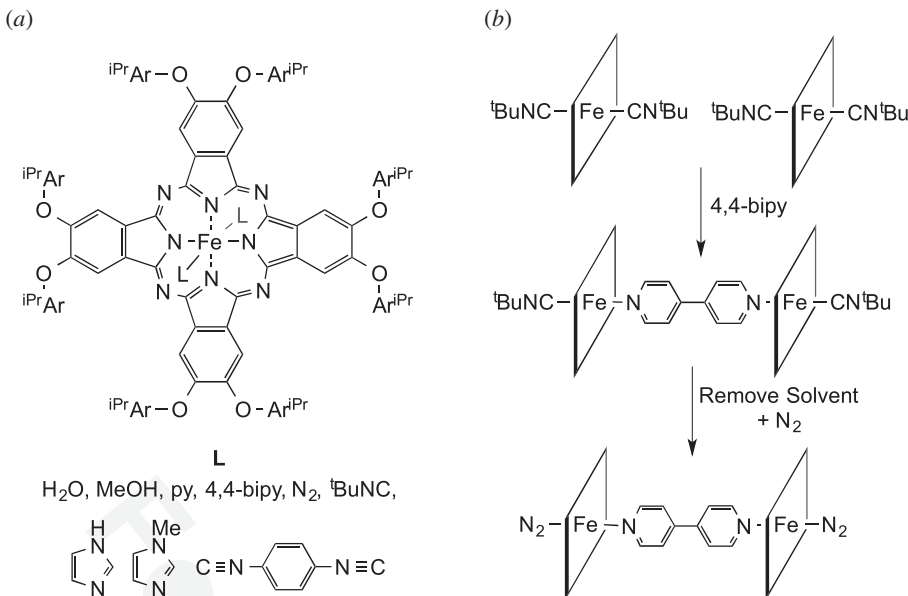
Scheme 10. Sequential SC–SC gas transfer transitions. Ar^{iPr} = 2,6-ⁱPr₂C₆H₃.

loss of crystallinity, albeit these processes occur in the microcrystalline powder state and the transformations are monitored by powder diffraction techniques and IR spectroscopy rather than by single-crystal X-ray diffraction (crystals suitable for such analysis were grown independently). The authors speculate that these processes are likely to involve local solutions of the reactants that recrystallize at a comparable rate to solute formation. They proposed that this material could be used as a gas-triggered switch, with SO₂ uptake signalled either by colour change or by crystal expansion. SC–SC transitions may also occur sequentially. In an elegant example, Crudden and co-workers [70] presented a double SC–SC gas exchange reaction using the (S^IPr)₂RhCl(L) system (S^IPr = N,N'-(2,6-ⁱPr₂C₆H₃)₂C₃H₄N₂, L=N₂, O₂ or CO; scheme 10). First, N₂ is replaced with O₂ to give a dioxygen adduct, and then O₂ is replaced with CO, without crystal degradation at either stage.

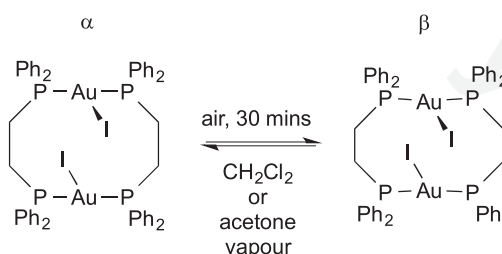
Alcohol uptake (i.e. MeOH, EtOH and iPrOH) by the non-porous coordination polymer [Ag₄(O₂C(CF₂)₂CF₃)₄(TMP)₃]_n (A) is reversible in a SC–SC transformation by a solid–vapour process (TMP = 2,3,5,6-tetramethylpyrazine). In an elegant sequence of substitution reactions, consecutive alcohols are introduced into the lattice: A-EtOH → A-MeOH → A-ⁱPrOH → A-EtOH without loss of single crystallinity. These ligand substitution reactions are accommodated by changes in coordination geometry at specific Ag(I) centres, and specifically alcohol insertion occurs into one-quarter of the Ag–O carboxylate bonds [73,74]. As this material does not have significant porosity, a mechanism is proposed in which concerted motion of the disordered fluoroalkyl chains allows for the transport of the alcohol molecules within the crystals. Powder X-ray crystallography techniques were also used to follow these transformations.

SC–SC transitions can also take place in a suspension of non-solvating liquid, for example in polymeric platform materials. McKeown and co-workers [33] reported such SC–SC transitions using Fe(MeOH)₂(phthalocyanine). Large interconnected voids (8 nm³) run through these structures that are defined by a cubic assembly of six of the phthalocyanine groups. These voids allow liquid penetration, and axial ligands can be reversibly, and rapidly, displaced by a variety of exogenous ligands (scheme 11). Interestingly, monodentate ligands bind preferentially to an axial binding site within this cubic assembly, whereas bidentate ligands selectively bind to link neighbouring cubic assemblies together. Selective exchange between water and methanol has been observed as a SC–SC transformation in the trinuclear iron complexes [Fe₃(μ₃-O)(μ₂-CH₃COO)₆(C₅H₅NO)₂(L)][ClO₄] (L=H₂O, MeOH) [75], whereas heterolytic dissociation of water at a bis(μ-oxo)divanadiumpolyoxometallate, which models the interactions of water with metal oxide surfaces, was found to occur as a SC–SC transformation.

In the absence of added reagents, SC–SC transitions can occur in the form of a simple phase change within the crystal lattice. Balch and co-workers [77] reported a reversible phase change when acetone or dichloromethane vapour is passed over a crystal of β-Au₂(μ-Ph₂PCH₂CH₂PPh₂)₂I₂ · (OCMe)₂, even though no additional solvent incorporation is observed. Two equivalents of acetone are present in both phases. The reverse reaction occurs if the crystal is left in air (scheme 12).



Scheme 11. (a) Porous phthalocyanine–derivative complex ($\text{PNC}[\nu\text{L}-\text{Fe}-\text{Cl}]$) which can undergo SC–SC ligand (**L**) exchanges when immersed in organic solvents. $\text{Ar}^{\text{Pr}} = 2,6\text{-}^{\text{t}}\text{Pr}_2\text{C}_6\text{H}_3$. (b) Example of two sequential ligand exchanges, displaying the linking of two metal centres by a bidentate ligand (phthalocyanine derivative simplified to a flat square).

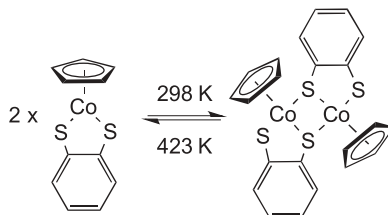


Scheme 12. Phase change SC–SC transition driven by drying in air and reversible by exposure to CH_2Cl_2 or acetone vapour.

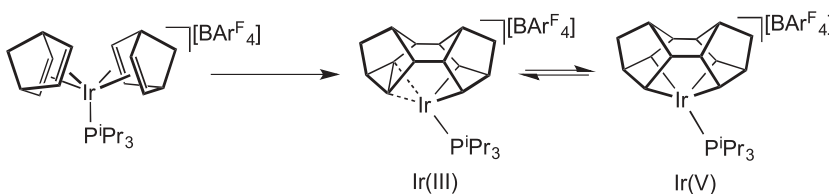
Brill, Rheingold and co-workers [78] of $(\eta^5\text{-C}_5\text{H}_5)\text{Co}(\text{S}_2\text{C}_6\text{H}_4)$ in the single-crystal phase at room temperature could be reversed upon warming to 423 K while still maintaining crystallinity (scheme 13). The dimeric species is thermodynamically favoured in the crystalline lattice at room temperature, but the monomer is favoured thermodynamically in solution, presumably owing to a dominant entropy term in solution.

Another SC–SC transformation that occurs without additional reagent is the reversible C–C activation in $[\text{Ir}(\text{BINOR-S})(\text{P}^{\text{i}}\text{Pr}_3)][\text{BAr}_4^{\text{F}}]$, which contains a rare example of an agostic $\text{M}\cdots\text{C-C}$ bond ($\text{BINOR-S} = 1,2,4,5,6,8\text{-dimetheno-s-indacene}$). In this complex, reversible C–C cleavage occurs to form an equilibrium mixture, in the crystalline phase, of dynamically disordered C–C activated $[\text{Ir}(\text{V})]$ and C–C agostic $[\text{Ir}(\text{III})]$ complexes—the ratio of which changes with temperature. Interestingly, the $[\text{Ir}(\text{BINOR-S})(\text{P}^{\text{i}}\text{Pr}_3)][\text{BAr}_4^{\text{F}}]$ complex is itself made from a solid-state organometallic reaction, where cyclodimerization of two norbornadiene ligands occurs to yield the BINOR-S ligand (scheme 14) [79].

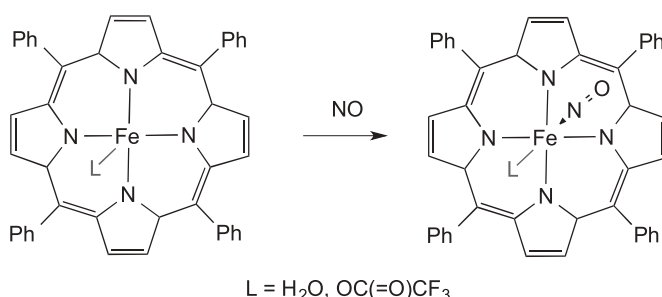
SC–SC reactions present possibilities for directly forming reactive complexes, which may not be accessible cleanly using solution routes. C–N oxidative cleavage in the PNP pincer



Scheme 13. Reversible dimerization in a single crystal.



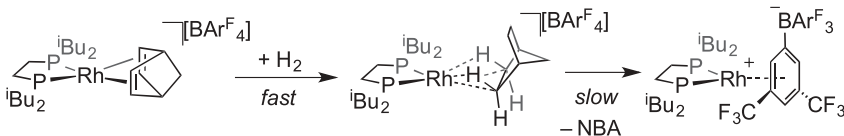
Scheme 14. Formation of a BINOR-S complex and reversible SC–SC C–C cleavage.



Scheme 15. Formation (NO)-Fe-porphyrin complexes by SC–SC transitions.

complex $\text{RhCl}[(^i\text{Pr}_2\text{P}(\text{C}_6\text{H}_3\text{Me}))_2\text{NMe}]$ to give $\text{Rh}(\text{Me})\text{Cl}[(^i\text{Pr}_2\text{P}(\text{C}_6\text{H}_3\text{Me}))_2\text{N}]$ occurs in the solid state in a SC–SC transformation [80]. Saliently, when performed in the bulk, this preparative route is cleaner than that in solution [81]. Richter-Addo and co-workers [82] were able to crystallographically characterize biologically important porphyrin complexes which bind NO. Examples include $(\text{TPP})\text{Fe}(\text{NO})(\text{OC}(=\text{O})\text{CF}_3)$, $[(\text{TPP})\text{Fe}(\text{NO})(\text{H}_2\text{O})][(\text{TPP})\text{Fe}(\text{H}_2\text{O})]\text{[OC}(=\text{O})\text{CF}_3]_2$ [83] (TPP = tetraphenylporphyrin) and $[(\text{oep})\text{Fe}(\text{NO})(\text{S}-2,6-(\text{CF}_3\text{CONH})_2\text{C}_6\text{H}_3)]$ [84] (oep = octaethylporphyrinato dianion). These complexes were formed by addition of NO gas to the unsaturated precursors in the solid state. This transformation was not possible using solution crystallization methods, as in solution a mixture of by-products form instead (scheme 15) [82–84].

Perhaps the most dramatic exploitation of solid-state SC–SC transformations in stabilizing highly reactive complexes comes from the addition of H_2 to the complex $[\text{Rh}(\text{NBD})(^i\text{Bu}_2\text{PCH}_2\text{CH}_2\text{P}^i\text{Bu}_2)][\text{BAr}_4^F]$ ($\text{NBD}=\text{C}_7\text{H}_8$, $\text{Ar}^F=3,5-\text{C}_6\text{H}_3(\text{CF}_3)_2$) that results in the isolation and structural characterization of a transition-metal sigma–alkane complex in which the hydrogenated organic fragment ($\text{NBA}=\text{C}_7\text{H}_{12}$) binds to the metal through two $\text{Rh}\cdots\text{H–C}$ sigma interactions $[\text{Rh}(\eta^2,\eta^2\text{-NBA})(^i\text{Bu}_2\text{PCH}_2\text{CH}_2\text{P}^i\text{Bu}_2)][\text{BAr}_4^F]$ (scheme 16) [85]. Such alkane complexes are exceedingly rare, with only two examples having been previously characterized in the solid state by single-crystal X-ray diffraction, in which there is a close approach of the alkane H–C bond to a metal centre [86,87]. Ultimately, this alkane complex undergoes a further



Scheme 16. Formation of an alkane complex in the solid state.

transformation, in the solid state, to form a complex in which the alkane ligand has been lost and the $[\text{BAr}_4^{\text{F}}]^-$ anion coordinates. An intermediate, mono-hydrogenated, species was proposed $[\text{Rh}(\eta^2(\text{CH}), \eta^2-(\text{C}=\text{C})(\text{NBE}))(\text{iBu}_2\text{PCH}_2\text{CH}_2\text{P}^{\text{l}}\text{Bu}_2)][\text{BAr}_4^{\text{F}}]$ ($\text{NBE} = \text{C}_7\text{H}_{10}$), which also adds H_2 in the solid state to give the alkane complex, as shown by solid state NMR spectroscopy.

(a) Overview of the structural changes associated with single-crystal-to-single-crystal transformations

Selected examples of SC–SC transitions are displayed in table 1 with their respective crystallographic volume change ($z = 1$ equivalent). Minimal structural changes are apparently necessary to allow for SC–SC transitions, and most examples reported show less than 4% volume change in the lattice volume. The outlier of van Koten and co-workers' example of SO_2 uptake is exceptional because it involves a very large percentage volume change (15.7%), with expansion predominantly along one axis. However, this occurs in the microcrystalline phase without loss of crystallinity as measured by powder diffraction, and SC–SC experiments were not successful. Noteworthy is the 10% change in volume associated with reversible alcohol addition in the Ag-carboxylates, this perhaps being associated with the fact that this material is a coordination polymer in the solid state, which might allow for increased flexibility without loss of crystallinity.

6. Catalysis in the solid state

(a) Heterogeneous organometallic catalysts

The heterogenization of single-site catalysts brings together the benefits of heterogeneous catalysis (i.e. recyclability and ease of removal from the reaction mixture) with the potential for intimate control over transformations that occur at the metal centre that is provided by the local ligand environment in a homogeneous system [15,16]. There are a number of strategies that can be used to facilitate the heterogenization of well-defined organometallic catalyst systems, including surface-supported organometallic chemistry in which a platform material such as silica, zeolites or metal oxides support directly, or indirectly via linker groups, the organometallic complex [88–98]. Metal organic frameworks (MOFs) are also particularly attractive as one-, two- and three-dimensional assemblies can be created in which the metal atoms often act as the geometry-enforcing linkage points, but can also be envisaged as potential active sites for catalysis [24]. In addition, a MOF may simply act as a reaction cavity, with the organometallic species as a host/guest material [99]. Within the context of this review that concentrates on the reactivity of well-defined organometallic complexes in the solid state these materials, as they are often not well defined at the metal centre of interest, are not included here.

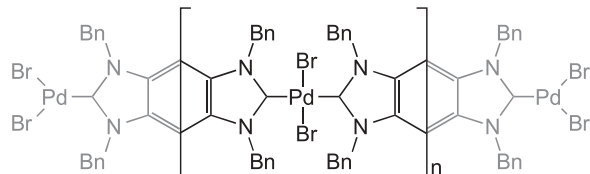
(b) Self-supported organometallic catalysis

Self-supported catalysts invoke an active metal centre in which the ligand environment also acts as the platform microporous material [100]. The advantage in many of these systems, compared with heterogenized organometallic catalysts, is that they are well defined at the

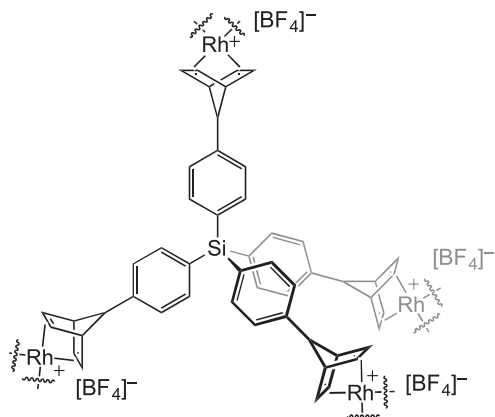
Table 1. Examples of SC–SC transitions and the crystallographic volume changes involved. POCOP = 1,3-[0P{C₆H₅(CF₃)₃-2,4,6]C₆H₅; NCN = C₆H₅-5-(OH)-1,3(CH₂NMe₂)₂; SPr = N,N'-(2,6-iPr₂C₆H₃)₂C₃H₅N₂; TPP = tetraphenylporphyrin; oep = octaethylporphyrinato dianion; NBD = C₇H₈; NBA = C₇H₁₂; Ar^F = 3,5-C₆H₃(CF₃)₂; TMP = 2,3,5,6-tetramethylpyrazine.

entry	starting complex space group, volume (Å ³), z	product space group, volume (Å ³), z	[change in volume (Å ³) and percentage change for z = 1 equivalent]
1 Brookhart and co-workers [13]	(POCOP)Ir(N ₂); $\bar{P} = 1,3002.1(4)$, z = 2	(POCOP)Ir(O ₂); $\bar{P} = 1,3046.3(10)$, z = 2	[+22] +1.4%
		(POCOP)Ir(CO); $\bar{P} = 1,30001(2)$, z = 2	[−1] −0.6%
		(POCOP)Ir(C ₆ H ₄); $\bar{P} = 1,3020.6(2)$, z = 2	[+9] +0.6%
		(POCOP)Ir(H ₂)(H ₂); $\bar{P} = 1,2986.6(4)$, z = 2	[−8] −0.6%
		(POCOP)Ir(NH ₃); $\bar{P} = 1,3033.56(9)$, z = 2	[+1] +0.04%
		(NCN)Pt(C ₁₀ O ₂); Pna2 ₁ , 15575(4), z = 4	[+33] +15.7%
2 van Koten and co-workers [7]	(NCN)PtCl ₂ Fe ²⁺ Na ₂ , 1346.0(4), z = 4	(SPt)RhCl(N ₂); P2 ₁ 2 ₁ 2, 2855.15(8), z = 2	[−3] −0.1%
3 Cradden and co-workers [70]	(SPt)RhCl(N ₂); P2 ₁ 2 ₁ 2, 2855.15(8), z = 2	(SPt)RhCl(O ₂); P2 ₁ 2 ₁ 2, 2861(3), z = 2	[+9] +0.4%
4 McKeown and co-workers [33]	(SPt)RhCl(O ₂); P2 ₁ 2 ₁ 2, 2852.13(12), z = 2	PNC[^c Bu ^b Nc ^c Fe ^d v ^e Bu ^f Nc ^g]Pn ^h −3n, 52348.5(7), z = 12	[+32] +0.7%
		PNC[^c Bu ^b Nc ^c Fe ^d v ^e (Py) _{0.7} [Bu ^f Nc ^g] _{0.3}]; Pn ^h −3n, 523736(2), z = 12	[+39] +0.8%
		PNC[MeOH ^b Fe ^c v ^e Mel(C ₃ N ₂ H ₃) ₂]; Pn ^h −3n, 52819.6(12), z = 12	[+160] +3.7%
		PNC[^c Bu ^b Nc ^c Fe ^d v ^e Bu ^f Nc ^g]; Pn ^h −3n, 54263.4(5), z = 12	[+71] +1.6%
5 Balch and co-workers [77]	α-Al ₂ (μ-Ph ₂ PC ₆ H ₃ Ph ₂) ₂ (OMe) ₂ ; P2 ₁ /c, 2824.28(3), z = 2	βAl ₂ (μ-Ph ₂ PC ₆ H ₃ Ph ₂) ₂ b ₂ (OMe) ₂ ; P = 1,141(997), z = 1	[−0.2] ~0%
6 Brill, Riehngold and co-workers [78]	(η ⁵ -C ₅ H ₅)Co(S ₂ C ₆ H ₄); P2 ₁ /c, 2159.1(6), z = 8	[η ⁵ -C ₅ H ₅]Co(S ₂ C ₆ H ₄); P2 ₁ /c, 1031.2(3), z = 2 (dimer)	[−12] −4.5% ^a
7 Richter-Addo and co-workers [82–84]	(TPP)Fe(C=O)(F ₃); P = 1,2093.1(3), z = 2	(TPP)Fe(C=O)(F ₃); P = 1,2144(3), z = 2	[+25] +2.4%
	[TPP]Fe(H ₂ O)][O(C=O)F ₃]; $\bar{P} = 1,1833.4(3)$, z = 2	[TPP]Fe(H ₂ O)][(TPPF(H ₂ O))][O(C=O)F ₃]; $\bar{P} = 1,3818.2(6)$, z = 2	[+38] +4.1% ^b
	[oep]FeS ₂ ·6-(C ₃ CONH) ₂ C ₆ H ₄]; $\bar{P} = 1,2266.3(6)$, z = 2	[oep]Fe(Ni)[S ₂ ·6-(C ₃ CONH) ₂ C ₆ H ₄]; $\bar{P} = 1,2360(2)$, z = 2	[+47] +4.1%
8 Weller and co-workers [85]	[Rh(Bip ₂ PC ₆ H ₃ Ph) ^b Bu ₂](η ² -NBD)[BAI] ₄ ^c ; C2/c, 5957.62(18), z = 4	Rh(Bip ₂ PC ₆ H ₃ Ph) ^b Bu ₂](η ² -NBAI)[BAI] ₄ ; C2/c, 6044(13), z = 4	[+22] +1.5%
9 Ozerov and co-workers [80, 81]	RhCl[(P ₂ P(C ₆ H ₅ Me) ₂ NMe) ₂] ₂ B ₂ Li ₂ , 595(4), z = 8	Rh(MeCl)[(P ₂ P(C ₆ H ₅ Me) ₂ Ni) ₂]P ₂ Li ₂ , 5976(4), z = 8	[+21] +0.4%
10 Brammer and co-workers [74]	[Ag ₄ O ₂ (CF ₃) ₂ Fe] ₄ [(TMP) ₃] _m ; $\bar{P} = 1,1405.34(6)$, z = 1	[Ag ₄ O ₂ (CF ₃) ₂ Fe] ₄ [(PbO) ₃]; $\bar{P} = 1,1545.9(2)$, z = 1	[+140.6] +0.0%

^a z = 1 monomer, z = 1/2 dimer. ^b z = 1 starting material, z = 1/2 product.



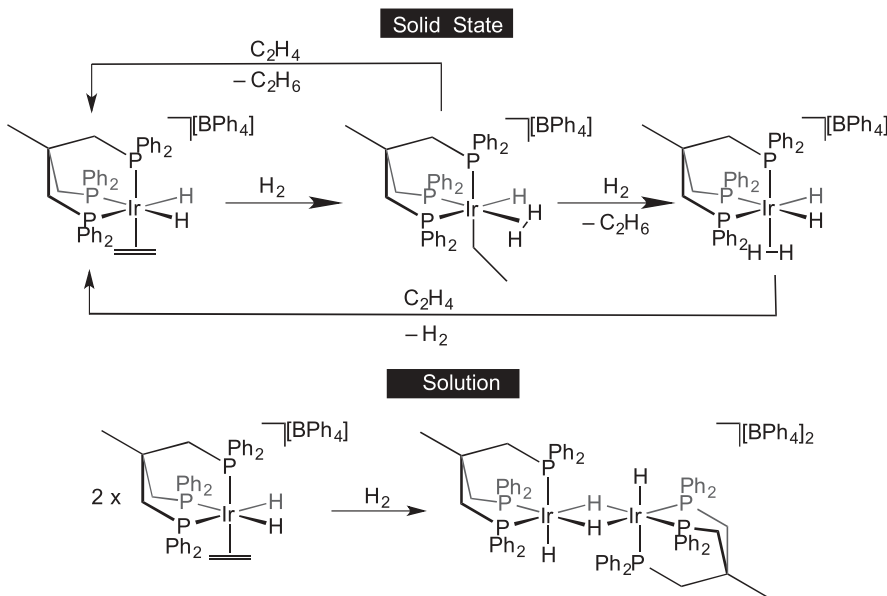
Scheme 17. A coordination polymer with Pd capable of catalysing heterogeneous Suzuki–Miyaura cross coupling in water.



Scheme 18. A microporous organometallic framework based upon rhodium alkene coordination.

metal–centre and thus more amenable to structural and spectroscopic investigation. Early reports of self-supported catalysts include the linkage polymers of $[\text{RhCl}(\text{CO})(1,4-(\text{CN})_2\text{C}_6\text{H}_4)]_n$ which can hydrogenate and isomerize 1-hexene, with no leaching of complexes into solution [101]. The active rhodium site was created by photolytic dissociation of the CO ligand. A similar system was formed with two bridging ligands per metal, enabling a well-defined three-dimensional-stacked layer structure to form. The surface and corner positions of this structure are likely to contain unsaturated metal centres which are catalytically active; however, the interior sites are proposed to be totally inactive [102,103]. Multi-dentate oxime, thiourea, phosphine and NHC ligands have been used to form frameworks with Pd-centres for use in Suzuki–Miyaura C–C coupling reactions [104–107]. For example, Karimi & Akhavan [107] reported a coordination polymer of palladium with a linking bidentate NHC ligand, which is insoluble in water, resulting in C–C coupling catalysis that could be performed using water as the substrate and product solvent (scheme 17). Although the authors used the mercury test, which probes for nanoparticle formation, which showed no loss in activity, it is difficult to unequivocally prove that nanoparticles are in no way involved for such systems.

More complex microporous structures can also be formed with a mixture of metal sites. For instance, copper, nickel or palladium porphyrin moieties can be combined with rhodium–polycarboxylate linkages in which both metal sites may exhibit cooperative effects for hydrogenation reactions [108,109]. Kaskel and co-workers [110] have recently reported the formation of a microporous organometallic network based upon a rhodium alkene fragment linked to a rigid tetraphenylsilane backbone (scheme 18). While an accurate structural determination has proved difficult, the framework appeared to be air-stable unlike its homogeneous analogue $[\text{Rh}(\text{NBD})_2][\text{BF}_4]$. This material catalysed transfer hydrogenation reactions.



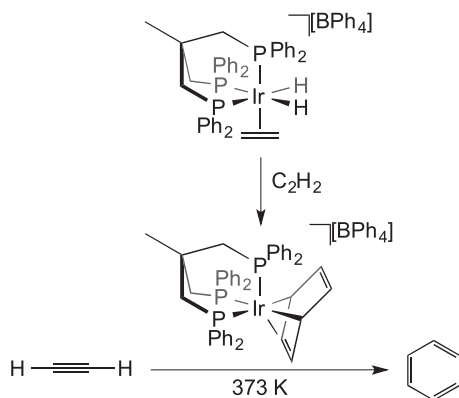
Scheme 19. Catalytic ethene hydrogenation in the solid state versus solution.

(c) Solid-state organometallic catalysis without a support

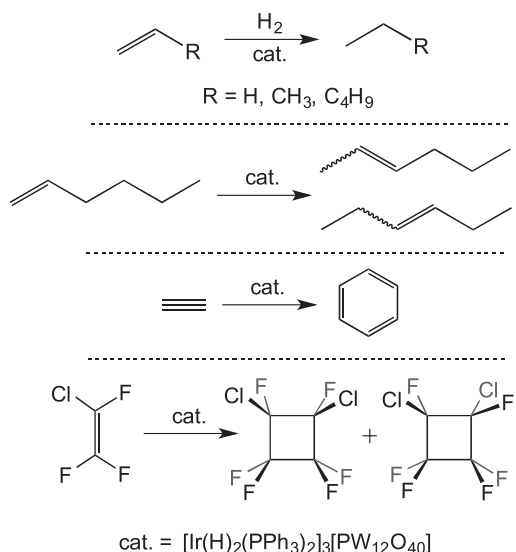
Solid-state catalysis using well-defined organometallic complexes that are not incorporated into a platform material is a relatively undeveloped field. Bianchini *et al.* [14] introduced the concept with simple ethene hydrogenation reactions using $[(\text{triphos})\text{Ir}(\text{H})_2(\text{C}_2\text{H}_4)]\text{[BPh}_4]$ at 343 K (scheme 19). The catalyst was active in the solid state, in a mechanism proposed to operate via hydride migration to form an $\text{Ir}-\text{(C}_2\text{H}_5)$ species, which can react with further H_2 followed by reductive elimination of ethane. In solution, the same species was not catalytically active, because a coordinatively saturated dimeric bridging hydride species rapidly forms in the presence of H_2 which was inactive for further reactions. Although some of the inactive dimeric species is also formed in the solid-state reaction, it appears to form at a slower rate than in solution. This highlights the ability of the solid state to maintain the integrity of the reactive species by playing a role in protecting them from deactivation pathways that require structural reorganization. The $[\text{BPh}_4]^-$ anions are proposed to create a hydrophobic lattice structure ideal for allowing the passage of small hydrocarbon gases. The catalytic trimerization of ethyne to form benzene was also investigated by Bianchini and co-workers, who showed that a η^4 -benzene complex (formed itself from a solid–gas reaction) is an active pre-catalyst active at 373 K in the solid state (scheme 20) [55].

Siedle & Newmark [56] reported the room temperature catalytic activity of iridium phosphine cations partnered with Keggin-type trianions, $[\text{Ir}(\text{H})_2(\text{PPh}_3)_2]_3[\text{PW}_{12}\text{O}_{40}]$ (scheme 21), with the hydrogenation of ethene, propene and 1-hexene demonstrated. The isomerization of 1-hexene to a mixture of *cis*- and *trans*-2-hexenes and 3-hexenes was also reported, presumably via reversible C–H activation accessing an allyl-iridium–hydride intermediate. The authors do not comment on the rates of reaction. Similar to the findings of Bianchini, addition of excess ethyne forms benzene in catalytic quantities, with an iridium–benzene complex expected to act as the pre-catalyst, although the reaction is reported to be slow. The catalytic dimerization of $\text{CF}_2=\text{CFCl}$ to *cis*- and *trans*-1,2-dichlorohexafluorocyclobutane complexes was also reported.

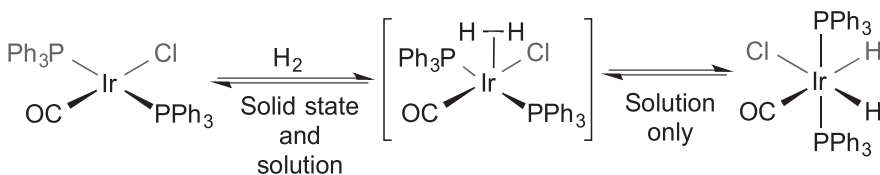
Limbach and co-workers [111] have reported on the solid-state catalysed hydrogenation of ethene using Vaska's complex, $\text{Ir}(\text{CO})\text{Cl}(\text{PPh}_3)_2$, by following the reaction products by gas-phase ^1H NMR spectroscopy. In solution, the product of H_2 addition (which presumably related to the



Scheme 20. Trimerization of ethyne using a solid-state catalyst.



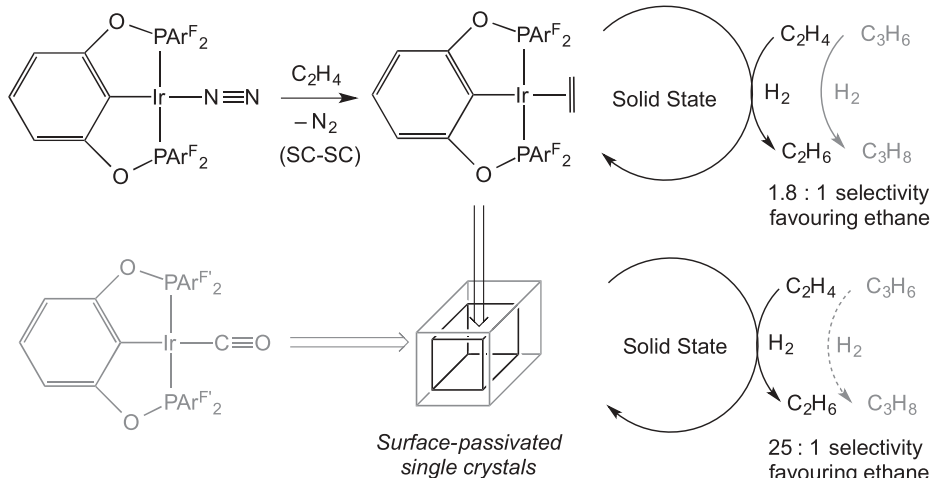
Scheme 21. Catalytic reactions using $[\text{Ir}(\text{H})_2(\text{PPh}_3)_2]_3[\text{PW}_{12}\text{O}_{40}]$.



Scheme 22. Reaction of Vaska's complex with H₂ in the solid state and solution.

active catalyst) is a *cis*-dihydride/*trans*-phosphine species. In the solid state, this is not formed, and it was proposed that this was due to ligand reorientation being inhibited. The authors thus suggested a different pathway for hydrogenation in the solid state and solution (**scheme 22**) that invokes a dihydrogen intermediate as the active species in the solid state.

Brookhart *et al.* [13] have reported the hydrogenation of ethene using single crystals of (POCOP)Ir(N₂), as monitored by gas-phase NMR spectroscopy. At 298 K, the reaction requires



Scheme 23. Hydrogenation of ethene using single crystals, and the selective hydrogenation of ethene in the presence of propene using surface-passivated single crystals.

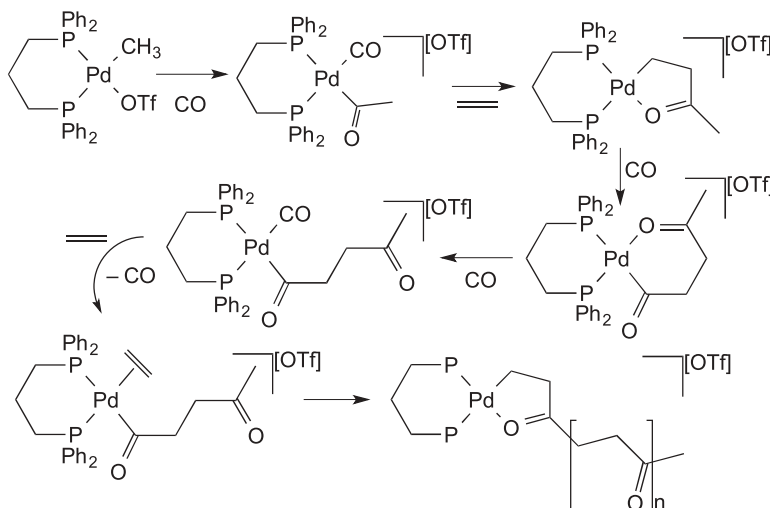
5 h to reach 95% conversion, but at 348 K 99% conversion occurs within 30 min. At this higher temperature, lattice-incorporated toluene is lost, and this is proposed to be responsible for the higher activity. (POCOP)Ir(C₂H₄) is the suggested resting state. Remarkable selective catalytic hydrogenation inside single crystals was also presented. By passivating the surface sites of crystals of (POCOP)Ir(N₂) with a layer of (POCOP)Ir(CO), an incomplete crystal-to-crystal transition occurs. The resulting material can selectively hydrogenate ethene in the presence of propene, with a 25 : 1 preference at 348 K (scheme 23) [13]. It was proposed that the porous crystals allow the smaller ethene and hydrogen molecules access to the active interior metal sites, whereas the larger propene molecules cannot penetrate the surface. In the absence of surface passivation, only a small selectivity is seen in favour of hydrogenation of ethene (1.8 : 1 ratio of ethane to propane produced at 298 K), consistent with this.

Mul and co-workers [112] have reported upon the palladium-catalysed CO/C₂H₄ co-polymerization reaction which is operated under gas phase or slurry conditions in industry. The catalyst becomes incorporated into the growing polymer chain, and so its nature as a heterogeneous or homogeneous catalyst is not well defined. Mul *et al.* chose to investigate the mechanism by using microcrystalline (Ph₂PCH₂CH₂CH₂PPh₂)Pd(CH₃)(OTf) deposited onto a gold surface. They were able to probe the first few turnovers of reaction using polarization modulation reflection-absorption IR spectroscopy (scheme 24). The findings suggest that ethene insertion into the Pd-acyl bond is actually CO-assisted. The incoming CO is able to displace the chelating ketone group more easily than ethene, but can itself then exchange with ethene. This subtlety had not been previously revealed by solution studies.

Dorta *et al.* [113] formed a variety of chiral crystalline organometallic complexes with either chiral phosphine ligands or chiral counterions, with the idea to investigate asymmetric catalysis. Unfortunately, this was not achieved, in this instance, and this interesting area has yet to be successfully developed.

7. Conclusion and future outlook

We hope that this review has shown that solid-state organometallic chemistry can offer significant advantages over the solution phase, especially when kinetic stability, or overall reaction selectivity, are different in the solid state compared with solution. Particularly exciting is the opportunity presented for SC-SC transformations in the solid state, as this methodology not



Scheme 24. The proposed mechanism for the copolymerization of CO and ethene using a palladium catalyst in the solid state.

only provides synthetic routes to new complexes but also enables direct structural analysis by single-crystal X-ray diffraction. However, for such transformations to proceed there is a requirement for minimal structural reorganization, and the appropriate design of systems that allow for this (e.g. large anions or bulky ligand groups) thus needs to be considered. An exciting prospect exists, which has not been developed to a significant extent, for such transformations to also result in catalytic processes. One example we suggest here is the selective transformation of hydrocarbons (alkane upgrading), where both solid–gas reactivity and selectivity from the local spatially well-defined environment will be important in producing effective and efficient catalysis. It will be fascinating to see how the field evolves as more examples of solid-state organometallic transformations are reported.

Acknowledgements. The EPSRC for funding SDP (EP/L505031/1).

References

- Hartwig JF. 2010 *Organotransition metal chemistry*. Sausalito, CA: University Science Books.
- Crabtree RH. 2005 *The organometallic chemistry of the transition metals*, 4th edn. Hoboken, NJ: John Wiley & Sons Inc.
- Bowker M. 1998 *Basis and applications of heterogeneous catalysis*. New York, NY: OUP.
- Smart LE, Moore EA. 2005 *Solid state chemistry: an introduction*, 3rd edn. New York, NY: CRC Press.
- Thomas JM, Thomas WJ. 2005 *Principles and practice of heterogeneous catalysis*, 3rd edn. Weinheim, Germany: VCH Publishers.
- Karunadasa HI, Montalvo E, Sun YJ, Majda M, Long JR, Chang CJ. 2012 A molecular MoS₂ edge site mimic for catalytic hydrogen generation. *Science* **335**, 698–702. (doi:10.1126/science.1215868)
- Halpern J. 1982 Mechanism and stereoselectivity of asymmetric hydrogenation. *Science* **217**, 401–407. (doi:10.1126/science.217.4558.401)
- Gonzalez-Rodriguez C, Pawley RJ, Chaplin AB, Thompson AL, Weller AS, Willis MC. 2011 Rhodium-catalyzed branched-selective alkyne hydroacylation: a ligand-controlled regioselectivity switch. *Angew. Chem. Int. Ed.* **50**, 5134–5138. (doi:10.1002/anie.201100956)
- Brookhart M, Green MLH, Parkin G. 2007 Agostic interactions in transition metal compounds. *Proc. Natl Acad. Sci. USA* **104**, 6908–6914. (doi:10.1073/pnas.0610747104)
- Strauss SH. 1993 The search for larger and more weakly coordinating anions. *Chem. Rev.* **93**, 927–942. (doi:10.1021/cr00019a005)

11. Verat AY, Pink M, Fan H, Tomaszewski J, Caulton KG. 2008 $[({}^t\text{Bu}_2\text{PCH}_2\text{SiMe}_2)_2\text{N}] \text{Rh(I)}$? Rapidly reversible H-C(sp³) and H-C(sp²) bond cleavage by rhodium(I). *Organometallics* **27**, 166–168. ([doi:10.1021/om701165n](https://doi.org/10.1021/om701165n))
12. Coville NJ, Cheng L. 1998 Organometallic chemistry in the solid state. *J. Organometal. Chem.* **571**, 149–169. ([doi:10.1016/s0022-328x\(98\)00914-0](https://doi.org/10.1016/s0022-328x(98)00914-0))
13. Huang Z, White PS, Brookhart M. 2010 Ligand exchanges and selective catalytic hydrogenation in molecular single crystals. *Nature* **465**, 598–601. ([doi:10.1038/nature09085](https://doi.org/10.1038/nature09085))
14. Bianchini C, Farnetti E, Graziani M, Kaspar J, Vizza F. 1993 Molecular solid–gas organometallic chemistry. Catalytic and stoichiometric transformations of ethyne at iridium. *J. Am. Chem. Soc.* **115**, 1753–1759. ([doi:10.1021/ja00058a021](https://doi.org/10.1021/ja00058a021))
15. Jones C. 2010 On the stability and recyclability of supported metal–ligand complex catalysts: myths, misconceptions and critical research needs. *Top. Catal.* **53**, 942–952. ([doi:10.1007/s11244-010-9513-9](https://doi.org/10.1007/s11244-010-9513-9))
16. Madhavan N, Jones CW, Weck M. 2008 Rational approach to polymer-supported catalysts: synergy between catalytic reaction mechanism and polymer design. *Acc. Chem. Res.* **41**, 1153–1165. ([doi:10.1021/ar800081y](https://doi.org/10.1021/ar800081y))
17. Tsoukala A, Peeva L, Livingston AG, Bjørsvik H-R. 2011 Separation of reaction product and palladium catalyst after a Heck coupling reaction by means of organic solvent nanofiltration. *Chem. Sus. Chem.* **5**, 188–193. ([doi:10.1002/cssc.201100355](https://doi.org/10.1002/cssc.201100355))
18. Hagen J. 1999 *Industrial catalysis: a practical approach*. Weinheim, Germany: Wiley-VCH.
19. Coville NJ, Levendis DC. 2002 Organometallic chemistry: structural isomerization reactions in confined environments. *Eur. J. Inorg. Chem.* **2002**, 3067–3078. ([doi:10.1002/1099-0682\(200212\)2002:12<3067::AID-EJIC3067>3.0.CO;2-4](https://doi.org/10.1002/1099-0682(200212)2002:12<3067::AID-EJIC3067>3.0.CO;2-4))
20. Hernández JG, Macdonald NAJ, Mottillo C, Butler IS, Friščík T. 2014 A mechanochemical strategy for oxidative addition: remarkable yields and stereoselectivity in the halogenation of organometallic Re(I) complexes. *Green Chem.* **16**, 1087–1092. ([doi:10.1039/c3gc42104j](https://doi.org/10.1039/c3gc42104j))
21. Egbert JD, Slawin AMZ, Nolan SP. 2013 Synthesis of N-heterocyclic carbene gold complexes using solution-phase and solid-state protocols. *Organometallics* **32**, 2271–2274. ([doi:10.1021/om301187a](https://doi.org/10.1021/om301187a))
22. Lewiński J, Dutkiewicz M, Lesiuk M, Śliwiński W, Zelga K, Justyniak I, Lipkowski J. 2010 Solid-state conversion of the solvated dimer $[({}^t\text{BuZn}(\mu-\text{O}^t\text{Bu})_2)]$ into a long overlooked trimeric $[({}^t\text{BuZnO}^t\text{Bu})_3]$ species. *Angew. Chem. Int. Ed.* **49**, 8266–8269. ([doi:10.1002/anie.201004504](https://doi.org/10.1002/anie.201004504))
23. Braga D, Giaffreda SL, Grepioni F, Pettersen A, Maini L, Curzi M, Polito M. 2006 Mechanochemical preparation of molecular and supramolecular organometallic materials and coordination networks. *Dalton Trans.* 1249–1263. ([doi:10.1039/B516165G](https://doi.org/10.1039/B516165G))
24. Furukawa H, Cordova KE, O’Keeffe M, Yaghi OM. 2013 The chemistry and applications of metal-organic frameworks. *Science* **341**, 1230444. ([doi:10.1126/science.1230444](https://doi.org/10.1126/science.1230444))
25. Liu J, Chen L, Cui H, Zhang J, Zhang L, Su C-Y. 2014 Applications of metal-organic frameworks in heterogeneous supramolecular catalysis. *Chem. Soc. Rev.* **43**, 6011–6061. ([doi:10.1039/C4CS00094C](https://doi.org/10.1039/C4CS00094C))
26. Hatcher LE, Raithby PR. 2013 Solid-state photochemistry of molecular photo-switchable species: the role of photocrystallographic techniques. *Acta Crystallogr. C* **69**, 1448–1456. ([doi:10.1107/S010827011303223X](https://doi.org/10.1107/S010827011303223X))
27. Coppens P. 2009 The new photocrystallography. *Angew. Chem. Int. Ed.* **48**, 4280–4281. ([doi:10.1002/anie.200900910](https://doi.org/10.1002/anie.200900910))
28. Inokuma Y, Kawano M, Fujita M. 2011 Crystalline molecular flasks. *Nat. Chem.* **3**, 349–358. ([doi:10.1038/nchem.1031](https://doi.org/10.1038/nchem.1031))
29. Horiuchi S, Murase T, Fujita M. 2012 A remarkable organometallic transformation on a cage-incarcerated dinuclear ruthenium complex. *Angew. Chem. Int. Ed.* **51**, 12 029–12 031. ([doi:10.1002/anie.201206325](https://doi.org/10.1002/anie.201206325))
30. Kawano M, Kobayashi Y, Ozeki T, Fujita M. 2006 Direct crystallographic observation of a coordinatively unsaturated transition-metal complex in situ generated within a self-assembled cage. *J. Am. Chem. Soc.* **128**, 6558–6559. ([doi:10.1021/ja0609250](https://doi.org/10.1021/ja0609250))
31. Bala MD, Coville NJ. 2007 Organometallic chemistry in the melt phase. *J. Organometal. Chem.* **692**, 709–730. ([doi:10.1016/j.jorganchem.2006.10.046](https://doi.org/10.1016/j.jorganchem.2006.10.046))
32. van der Boom ME. 2011 Consecutive molecular crystalline-state reactions with metal complexes. *Angew. Chem. Int. Ed.* **50**, 11 846–11 848. ([doi:10.1002/anie.201105940](https://doi.org/10.1002/anie.201105940))

33. Bezzu CG, Helliwell M, Warren JE, Allan DR, McKeown NB. 2010 Heme-like coordination chemistry within nanoporous molecular crystals. *Science* **327**, 1627–1630. (doi:10.1126/science.1184228)
34. Cohen MD, Schmidt GMJ. 1964 383. Topochemistry. Part I. A survey. *J. Chem. Soc.* 1996–2000. (doi:10.1039/jr9640001996)
35. Braga D. 1992 Dynamical processes in crystalline organometallic complexes. *Chem. Rev.* **92**, 633–665. (doi:10.1021/cr00012a007)
36. Sakamoto M. 1997 Absolute asymmetric synthesis from achiral molecules in the chiral crystalline environment. *Chem. Eur. J.* **3**, 684–689. (doi:10.1002/chem.19970030506)
37. Kaupp G. 1996 *Comprehensive supramolecular chemistry* (eds JL Atwood, JED Davies, DD MacNicol, F Votgle). New York, NY: Pergamon.
38. Oliván M, Marchenko AV, Coalter JN, Caulton KG. 1997 Gas/solid reactivity of unsaturated ruthenium-containing molecular solids. *J. Am. Chem. Soc.* **119**, 8389–8390. (doi:10.1021/ja971608j)
39. Vaska L. 1966 Stereospecific addition of hydrogen halides to tetragonal d⁸ complexes. *J. Am. Chem. Soc.* **88**, 5325–5327. (doi:10.1021/ja00974a055)
40. Cook PM, Dahl LF, Hopgood D, Jenkins RA. 1973 Oxidative-addition reaction of platinum acetylacetonate with iodine in solid state and solution. Crystal structure and equilibrium studies of trans-bis(acetylacetonato)di-iodoplatinum(IV). *J. Chem. Soc. Dalton Trans.* 294–301. (doi:10.1039/dt9730000294)
41. Vitorica-Yrezabal IJ, Sullivan RA, Purver SL, Curfs C, Tang CC, Brammer L. 2011 Synthesis and polymorphism of (4-ClpyH)₂[CuCl₄]: solid–gas and solid–solid reactions. *CrystEngComm* **13**, 3189–3196. (doi:10.1039/c0ce00628a)
42. Minguez Espallargas G, Florence AJ, van de Streek J, Brammer L. 2011 Different structural destinations: comparing reactions of [CuBr₂(3-Brpy)₂] crystals with HBr and HCl gas. *CrystEngComm* **13**, 4400–4404. (doi:10.1039/c1ce05222e)
43. Minguez Espallargas G, van de Streek J, Fernandes P, Florence AJ, Brunelli M, Shankland K, Brammer L. 2010 Mechanistic insights into a gas–solid reaction in molecular crystals: the role of hydrogen bonding. *Angew. Chem. Int. Ed.* **49**, 8892–8896. (doi:10.1002/anie.201003265)
44. Bianchini C, Peruzzini M, Zanobini F. 1991 Solid-state organometallic chemistry of tripodal (polyphosphine)metal complexes. Carbon–hydrogen activation reactions at cobalt(I) encapsulated into the tetraphosphine P(CH₂CH₂PPh₂)₃. *Organometallics* **10**, 3415–3417. (doi:10.1021/om00056a002)
45. Werner H, Rappert T, Baum M, Stark A. 1993 Metallorganische chemie in fester phase: umlagerungs-, eliminierungs- und additionsreaktionen von organometallverbindungen ohne solvens. *J. Organometal. Chem.* **459**, 319–323. (doi:10.1016/0022-328X(93)86085-V)
46. Jeffrey JC, Rauchfuss TB. 1979 Metal complexes of hemilabile ligands. Reactivity and structure of dichlorobis(o-(diphenylphosphino)anisole)ruthenium(II). *Inorg. Chem.* **18**, 2658–2666. (doi:10.1021/ic50200a004)
47. Braunstein P, Naud F. 2001 Hemilability of hybrid ligands and the coordination chemistry of oxazoline-based systems. *Angew. Chem. Int. Ed.* **40**, 680–699. (doi:10.1002/1521-3773(20010216)40:4<680::AID-ANIE6800>3.0.CO;2-0)
48. Osakada K, Ishii H. 2004 Solid–gas carbonylation of aryloxide rhodium(I) complexes: stepwise reaction forming Vaska-type complexes. *Inorg. Chim. Acta* **357**, 3007–3013. (doi:10.1016/j.ica.2004.02.030)
49. Chin CS, Lee B, Kim S. 1993 Solid-state reactions of iridium (I)-1,5-cyclooctadiene compounds with carbon monoxide: synthesis of cationic (1,5-cyclooctadiene)carbonyliridium (I) complexes. *Organometallics* **12**, 1462–1466. (doi:10.1021/om00028a077)
50. Gaviglio C, Ben-David Y, Shimon LJW, Doctorovich F, Milstein D. 2009 Synthesis, structure, and reactivity of nitrosyl pincer-type rhodium complexes. *Organometallics* **28**, 1917–1926. (doi:10.1021/om8011536)
51. Flynn BR, Vaska L. 1974 Reversible addition of carbon dioxide to rhodium and iridium complexes. *J. Chem. Soc. Chem. Commun.* 703–704. (doi:10.1039/c39740000703)
52. Truscott BJ, Nelson DJ, Slawin AMZ, Nolan SP. 2014 CO₂ fixation employing an iridium(I)-hydroxide complex. *Chem. Commun.* **50**, 286–288. (doi:10.1039/C3CC46922K)
53. Durr S, Zarzycki B, Ertler D, Ivanovic-Burmazovic I, Radius U. 2012 Aerobic CO oxidation of a metal-bound carbonyl in a NHC-stabilized cobalt half-sandwich complex. *Organometallics* **31**, 1730–1742. (doi:10.1021/om201037w)

54. Bianchini C, Frediani P, Graziani M, Kaspar J, Meli A, Peruzzini M, Vizza F. 1993 Molecular solid–gas organometallic chemistry. Catalytic and stoichiometric transformations of ethyne at iridium. *Organometallics* **12**, 2886–2887. (doi:10.1021/om00032a006)
55. Bianchini C, Graziani M, Kaspar J, Meli A, Vizza F. 1994 Molecular solid–gas organometallic chemistry. Catalytic and stoichiometric iridium-assisted C–C bond-forming reactions involving ethyne and ethene. *Organometallics* **13**, 1165–1173. (doi:10.1021/om00016a020)
56. Siedle AR, Newmark RA. 1989 Solid-state chemistry of molecular metal oxide clusters. Reactions of microporous dihydridobis(triphenylphosphine)iridium-tungsten complex $[(\text{Ph}_3\text{P})_2\text{IrH}_2]_3\text{PW}_{12}\text{O}_{40}$ with small organic molecules. *Organometallics* **8**, 1442–1450. (doi:10.1021/om00108a012)
57. Nicasio MC *et al.* 1999 Substitution and hydrogenation reactions on rhodium(I)-ethylene complexes of the hydrotris(pyrazolyl)borate ligands Tp' ($\text{Tp}'=\text{Tp}$, TpMe_2). *Inorg. Chem.* **39**, 180–188. (doi:10.1021/ic990419u)
58. Zenkina O, Altman M, Leitus G, Shimon LJW, Cohen R, van der Boom ME. 2007 From azobenzene coordination to aryl-halide bond activation by platinum. *Organometallics* **26**, 4528–4534. (doi:10.1021/om700519v)
59. Pike SD, Weller AS. 2013 C–Cl activation of the weakly coordinating anion $[\text{B}(3,5-\text{Cl}_2\text{C}_6\text{H}_3)_4]$ - at a Rh(I) centre in solution and the solid-state. *Dalton Trans.* **42**, 12832–12835. (doi:10.1039/c3dt51617b)
60. de los Rios I, Bustelo E, Puerta MC, Valerga P. 2010 Isomerization of internal alkynes to vinylidenes in tris(pyrazolyl)borate ruthenium complexes. Solution and solid-state kinetics. *Organometallics* **29**, 1740–1749. (doi:10.1021/om100084x)
61. Douglas TM, Weller AS. 2008 Acceptorless, intramolecular, alkyl dehydrogenation in the solid-state in a rhodium phosphine complex; reversible uptake of three equivalents of H_2 per molecule. *N. J. Chem.* **32**, 966–969. (doi:10.1039/B718615K)
62. Mediati M, Tachibana GN, Jensen CM. 1992 Solid-state and solution dynamics of the reversible loss of hydrogen from the iridium nonclassical polyhydride complexes $\text{IrClH}_2(\text{PR}_3)_2(\text{H}_2)$ ($\text{R}=\text{iso-Pr}$, Cy, tert-Bu). *Inorg. Chem.* **31**, 1827–1832. (doi:10.1021/ic00036a020)
63. Arif AM, Heaton DE, Jones RA, Kidd KB, Wright TC, Whittlesey BR, Atwood JL, Hunter WE, Zhang H. 1987 Synthesis and structures of di- and trinuclear di-tert-butylphosphido and di-tert-butylarsenido complexes of iridium. X-ray crystal structures of $[\text{Ir}(\mu\text{-tert-Bu}_2\text{E})(\text{CO})_2]_2$ ($\text{E}=\text{P}$, As), $[\text{Ir}(\text{tert-Bu}_2\text{PH})(\text{CO})_2]_2(\mu\text{-H})(\mu\text{-tert-Bu}_2\text{P})$, $[\text{Ir}(\text{tert-Bu}_2\text{PH})(\text{CO})(\mu\text{-H})_2]_2(\text{H})(\mu\text{-tert-Bu}_2\text{P})$, and $\text{Ir}_3(\mu\text{-tert-Bu}_2\text{P})_3(\text{CO})_5$. *Inorg. Chem.* **26**, 4065–4073. (doi:10.1021/ic00271a020)
64. Morris RH, Foley HC, Targas TS, Geoffroy GL. 1981 Photoinduced elimination of hydrogen from $[\text{Pt}_2\text{H}_3(\text{dppm})_2]\text{PF}_6$ and $[\text{Pt}_2\text{H}_2\text{Cl}(\text{dppm})_2]\text{PF}_6$. *J. Am. Chem. Soc.* **103**, 7337–7339. (doi:10.1021/ja00414a050)
65. Brayshaw SK, Ingleson MJ, Green JC, McIndoe JS, Raithby PR, Kociok-Köhn G, Weller AS. 2006 High hydride count rhodium octahedra, $[\text{Rh}_6(\text{PR}_3)_6\text{H}_{12}][\text{BAR}_4^{\text{F}}]_2$: synthesis, structures, and reversible hydrogen uptake under mild conditions. *J. Am. Chem. Soc.* **128**, 6247–6263. (doi:10.1021/ja0604663)
66. Goodfellow RJ, Hamon EM, Howard JA, Spencer JL, Turner DG. 1984 Cationic platinum hydride clusters: X-ray crystal structures of $[\text{Pt}_4\text{H}_2(\text{PBu}_3^{\text{t}})_4][\text{BF}_4]_2$ and $[\text{Pt}_4\text{H}_7(\text{PBu}_3^{\text{t}})_4][\text{BPh}_4]$. *J. Chem. Soc. Chem. Commun.* 1604–1606. (doi:10.1039/C3940001604)
67. Brayshaw SK, Ingleson MJ, Green JC, Raithby PR, Kociok-Köhn G, McIndoe JS, Weller AS. 2005 Holding onto lots of hydrogen: a 12-hydride rhodium cluster that reversibly adds two molecules of H_2 . *Angew. Chem. Int. Ed.* **44**, 6875–6878. (doi:10.1002/anie.200502221)
68. Aime S, Dastur W, Gobetto R, Krause J, Sappa E. 1995 Solid–gas reactions of the ‘lightly stabilized’ $\text{Os}_3(\text{CO})_{11}\text{L}$ ($\text{L}=\text{NCCH}_3$, C_2H_4) clusters with CO, NH_3 , and H_2 . *Organometallics* **14**, 3224–3228. (doi:10.1021/om00007a024)
69. Gemel C, Huffman JC, Caulton KG, Mauthner K, Kirchner K. 2000 Solution and solid–gas reactivity of unsaturated $[\text{RuCp}(\text{tmida})] +$ ($\text{tmida} = \text{Me}_2\text{NC}_2\text{H}_4\text{NMe}_2$). *J. Organometal. Chem.* **593**, 342–353. (doi:10.1016/S0022-328X(99)00545-8)
70. Zenkina OV, Keske EC, Wang R, Crudden CM. 2011 Double single-crystal-to-single-crystal transformation and small-molecule activation in rhodium NHC complexes. *Angew. Chem. Int. Ed.* **50**, 8100–8104. (doi:10.1002/anie.201103316)

71. Albrecht M, Lutz M, Spek AL, van Koten G. 2000 Organoplatinum crystals for gas-triggered switches. *Nature* **406**, 970–974. (doi:10.1038/35023107)
72. Albrecht M, Lutz M, Schreurs AMM, Lutz ETH, Spek AL, van Koten G. 2000 Self-assembled organoplatinum(II) supermolecules as crystalline, SO₂ gas-triggered switches. *J. Chem. Soc. Dalton Trans.* 3797–3804. (doi:10.1039/b006419j)
73. Libri S *et al.* 2008 Ligand substitution within nonporous crystals of a coordination polymer: elimination from and insertion into Ag–O bonds by alcohol molecules in a solid–vapor reaction. *Angew. Chem. Int. Ed.* **47**, 1693–1697. (doi:10.1002/anie.200703194)
74. Vitorica-Yrezabal IJ, Mínguez Espallargas G, Soleimannejad J, Florence AJ, Fletcher AJ, Brammer L. 2013 Chemical transformations of a crystalline coordination polymer: a multi-stage solid–vapour reaction manifold. *Chem. Sci.* **4**, 696. (doi:10.1039/c2sc21654j)
75. Supriya S, Das SK. 2007 Reversible single crystal to single crystal transformation through Fe–O(H)Me/Fe–OH₂ bond formation/bond breaking in a gas-solid reaction at an ambient condition. *J. Am. Chem. Soc.* **129**, 3464–3465. (doi:10.1021/ja067572p)
76. Uehara K, Mizuno N. 2011 Heterolytic dissociation of water demonstrated by crystal-to-crystal core interconversion from (μ -oxo)divanadium to bis(μ -hydroxo)divanadium substituted polyoxometalates. *J. Am. Chem. Soc.* **133**, 1622–1625. (doi:10.1021/ja108245g)
77. Lim SH, Olmstead MM, Balch AL. 2013 Inorganic topochemistry. Vapor-induced solid state transformations of luminescent, three-coordinate gold(I) complexes. *Chem. Sci.* **4**, 311–318. (doi:10.1039/c2sc20820b)
78. Miller EJ, Brill TB, Rheingold AL, Fultz WC. 1983 A reversible chemical reaction in a single crystal. The dimerization of η^5 -cyclopentadienyl(o-dithiobenzene)cobalt [CpCo(S₂C₆H₄-o)]. *J. Am. Chem. Soc.* **105**, 7580–7584. (doi:10.1021/ja00364a020)
79. Chaplin AB, Green JC, Weller AS. 2011 C–C activation in the solid state in an organometallic σ -complex. *J. Am. Chem. Soc.* **133**, 13 162–13 168. (doi:10.1021/ja2047599)
80. Ozerov OV, Guo C, Papkov VA, Foxman BM. 2004 Facile oxidative addition of N–C and N–H bonds to monovalent rhodium and iridium. *J. Am. Chem. Soc.* **126**, 4792–4793. (doi:10.1021/ja049659l)
81. Weng W, Guo C, Moura C, Yang L, Foxman BM, Ozerov OV. 2005 Competitive activation of N–C and C–H bonds of the PNP framework by monovalent rhodium and iridium. *Organometallics* **24**, 3487–3499. (doi:10.1021/om050346o)
82. Xu N, Goodrich LE, Lehnert N, Powell DR, Richter-Addo GB. 2013 Preparation of the elusive [(por)Fe(NO)(O-ligand)] complex by diffusion of nitric oxide into a crystal of the precursor. *Angew. Chem. Int. Ed.* **52**, 3896–3900. (doi:10.1002/anie.201208063)
83. Xu N, Powell DR, Richter-Addo GB. 2011 Nitrosylation in a crystal: remarkable movements of iron porphyrins upon binding of nitric oxide. *Angew. Chem. Int. Ed.* **50**, 9694–9696. (doi:10.1002/anie.201103329)
84. Xu N, Powell DR, Cheng L, Richter-Addo GB. 2006 The first structurally characterized nitrosyl heme thiolate model complex. *Chem. Commun.* 2030–2032. (doi:10.1039/b602611g)
85. Pike SD, Thompson AL, Algarra ASG, Apperley DC, Macgregor SA, Weller AS. 2012 Synthesis and characterization of a rhodium(I) σ -alkane complex in the solid state. *Science* **337**, 1648–1651. (doi:10.1126/science.1225028)
86. Evans DR, Drovetskaya T, Bau R, Reed CA, Boyd PDW. 1997 Heptane coordination to an iron(II) porphyrin. *J. Am. Chem. Soc.* **119**, 3633–3634. (doi:10.1021/ja970008h)
87. Castro-Rodriguez I, Nakai H, Gantzel P, Zakharov LN, Rheingold AL, Meyer K. 2003 Evidence for alkane coordination to an electron-rich uranium center. *J. Am. Chem. Soc.* **125**, 15 734–15 735. (doi:10.1021/ja0379316)
88. Basset JM, Lefebvre F, Santini C. 1998 Surface organometallic chemistry: some fundamental features including the coordination effects of the support. *Coord. Chem. Rev.* **178**, 1703–1723. (doi:10.1016/s0010-8545(98)00159-3)
89. Copéret C, Basset JM. 2007 Strategies to immobilize well-defined olefin metathesis catalysts: supported homogeneous catalysis vs. surface organometallic chemistry. *Adv. Syn. Catal.* **349**, 78–92. (doi:10.1002/adsc.200600443)
90. Staub H, Guillet-Nicolas R, Even N, Kayser L, Kleitz F, Fontaine F-G. 2011 Substantiating the influence of pore surface functionalities on the stability of Grubbs catalyst in mesoporous SBA-15 silica. *Chem. Eur. J.* **17**, 4254–4265. (doi:10.1002/chem.201002740)

91. Serna P, Gates BC. 2011 A bifunctional mechanism for ethene dimerization: catalysis by rhodium complexes on zeolite HY in the absence of halides. *Angew. Chem. Int. Ed.* **50**, 5528–5531. (doi:10.1002/anie.201008086)
92. Bhirud VA, Ehresmann JO, Kletnieks PW, Haw JF, Gates BC. 2005 Rhodium complex with ethylene ligands supported on highly dehydroxylated MgO: synthesis, characterization, and reactivity. *Langmuir* **22**, 490–496. (doi:10.1021/la052268f)
93. Gajan D, Coperet C. 2011 Silica-supported single-site catalysts: to be or not to be? A conjecture on silica surfaces. *N. J. Chem.* **35**, 2403–2408. (doi:10.1039/c1nj20506d)
94. Samantaray MK *et al.* 2013 Evidence for metal-surface interactions and their role in stabilizing well-defined immobilized Ru-NHC alkene metathesis catalysts. *J. Am. Chem. Soc.* **135**, 3193–3199. (doi:10.1021/ja311722k)
95. Thomas JM, Maschmeyer T, Johnson BFG, Shephard DS. 1999 Constrained chiral catalysts. *J. Mol. Catal. A, Chem.* **141**, 139–144. (doi:10.1016/S1381-1169(98)00257-X)
96. Thomas JM, Raja R. 2008 Exploiting nanospace for asymmetric catalysis: confinement of immobilized, single-site chiral catalysts enhances enantioselectivity. *Acc. Chem. Res.* **41**, 708–720. (doi:10.1021/ar700217y)
97. Hu A, Ngo HL, Lin W. 2003 Chiral, porous, hybrid solids for highly enantioselective heterogeneous asymmetric hydrogenation of β -keto esters. *Angew. Chem. Int. Ed.* **42**, 6000–6003. (doi:10.1002/anie.200351264)
98. Hu A, Ngo HL, Lin W. 2003 Chiral porous hybrid solids for practical heterogeneous asymmetric hydrogenation of aromatic ketones. *J. Am. Chem. Soc.* **125**, 11490–11491. (doi:10.1021/ja0348344)
99. Genna DT, Wong-Foy AG, Matzger AJ, Sanford MS. 2013 Heterogenization of homogeneous catalysts in metal-organic frameworks via cation exchange. *J. Am. Chem. Soc.* **135**, 10586–10589. (doi:10.1021/ja402577s)
100. Wang Z, Chen G, Ding K. 2008 Self-supported catalysts. *Chem. Rev.* **109**, 322–359. (doi:10.1021/cr800406u)
101. Efraty A, Feinstein I. 1982 Catalytic hydrogenation and isomerization of 1-hexene with $[\text{RhCl}(\text{CO})(1,4-(\text{CN})_2\text{C}_6\text{H}_4)]_n$ in the dark and under irradiation. *Inorg. Chem.* **21**, 3115–3118. (doi:10.1021/ic00138a038)
102. Feinstein-Jaffe I, Efraty A. 1987 Heterogeneous catalysis with coordination polymers: hydrogenation and isomerization of 1-hexene in the presence of $[\text{Rh}(\text{diisocyanobiphenyl})_2\text{Cl}]_n$. *J. Mol. Catal.* **40**, 1–7. (doi:10.1016/0304-5102(87)80001-9)
103. Lawrence SA, Sermon PA, Feinstein-Jaffe I. 1989 An investigation into the role of cooperative effects in polymeric rhodium(I) bis-4,4'-diisocyanobiphenyl chloride catalysts in olefin hydrogenation reactions. *J. Mol. Catal.* **51**, 117–127. (doi:10.1016/0304-5102(89)80092-6)
104. Liu Q-P, Chen Y-C, Wu Y, Zhu J, Deng J-G. 2006 Self-supported heterogeneous star-shaped oxime-palladacycle catalysts for the Suzuki coupling reactions. *Synlett* **2006**, 1503–1506. (doi:10.1055/s-2006-941585)
105. Chen W, Li R, Wu Y, Ding L-S, Chen Y-C. 2006 Self-supported thiourea-palladium complexes: highly air-stable and recyclable catalysts for the Suzuki reaction in neat water. *Synthesis* **2006**, 3058–3062. (doi:10.1055/s-2006-942531)
106. Yamada YMA, Maeda Y, Uozumi Y. 2006 Novel 3D coordination palladium network complex: a recyclable catalyst for Suzuki–Miyaura reaction. *Org. Lett.* **8**, 4259–4262. (doi:10.1021/o10615026)
107. Karimi B, Akhavan PF. 2009 Main-chain NHC-palladium polymer as a recyclable self-supported catalyst in the Suzuki–Miyaura coupling of aryl chlorides in water. *Chem. Commun.* 3750–3752. (doi:10.1039/b902096a)
108. Mori W, Sato T, Ohmura T, Nozaki Kato C, Takei T. 2005 Functional microporous materials of metal carboxylate: gas-occlusion properties and catalytic activities. *J. Solid State Chem.* **178**, 2555–2573. (doi:10.1016/j.jssc.2005.07.009)
109. Sato T, Mori W, Kato CN, Yanaoka E, Kuribayashi T, Ohtera R, Shiraishi Y. 2005 Novel microporous rhodium(II) carboxylate polymer complexes containing metalloporphyrin: syntheses and catalytic performances in hydrogenation of olefins. *J. Catal.* **232**, 186–198. (doi:10.1016/j.jcat.2005.02.007)
110. Stoeck U, Nicklerl G, Burkhardt U, Senkovska I, Kaskel S. 2012 Modular construction of a porous organometallic network based on rhodium olefin complexation. *J. Am. Chem. Soc.* **134**, 17335–17337. (doi:10.1021/ja305482a)

111. Matthes J, Pery T, Gründemann S, Buntkowsky G, Sabo-Etienne S, Chaudret B, Limbach H-H. 2004 Bridging the gap between homogeneous and heterogeneous catalysis: ortho/para H₂ conversion, hydrogen isotope scrambling, and hydrogenation of olefins by Ir(CO)Cl(PPh₃)₂. *J. Am. Chem. Soc.* **126**, 8366–8367. (doi:10.1021/ja0475961)
112. Mul WP, Oosterbeek H, Beitel GA, Kramer G-J, Drent E. 2000 *In situ* monitoring of a heterogeneous palladium-based polyketone catalyst. *Angew. Chem. Int. Ed.* **39**, 1848–1851. (doi:10.1002/(sici)1521-3773(20000515)39:10<1848::aid-anie1848>3.0.co;2-8)
113. Dorta R, Shimon L, Milstein D. 2004 Rhodium complexes with chiral counterions: achiral catalysts in chiral matrices. *J. Organometal. Chem.* **689**, 751–758. (doi:10.1016/j.jorgancchem.2003.12.012)